

---

Energy and the Environment Capstone Design Project  
Bass Connections 2017-2018

# Collapsible Electric Longboard

Jie Cai, *Computer Science '20*  
Tara Davis, *Mechanical Engineering '18*  
Ismail Iberkak, *Mechanical Engineering '18*  
Philemon Kiptoo, *Civil Engineering '18*  
Maya Patel, *Mechanical Engineering '18*  
Joe Squillace, *Computer Science '18*  
Houston Warren, *Statistical Science '18*

Spring 2018

---

|   |           |
|---|-----------|
| <b>1. Introduction</b>                    | <b>1</b>  |
| <b>2. Technical Design</b>                | <b>2</b>  |
| 2.1. Mechanical .....                     | 2         |
| 2.2. Software .....                       | 11        |
| <b>3. Societal Impact</b>                 | <b>17</b> |
| 3.1. Environmental Benefit Analysis ..... | 18        |
| 3.2. Social Benefit Analysis .....        | 19        |
| <b>4. Business Plan</b>                   | <b>22</b> |
| <b>5. Other Considerations</b>            | <b>25</b> |
| <b>6. Conclusion</b>                      | <b>25</b> |
| <b>7. Appendices</b>                      | <b>28</b> |



# Executive Summary

This report documents our team's completed Bass Connections in Energy Project on designing a collapsible electric longboard paired with a smartphone application. The goal of the project was to add portability, stronger environmental motivation, and a better overall user experience to the electric longboard market, which targets millennial commuters looking to save time, energy, and the environment. Our proposed business plan to make all components open-source makes the product simple for users to make themselves, while also being a cheaper alternative to brand name electric longboards. Not only does the product lend well to the growing electric longboarding do-it-yourself community, but also provides additional incentive to invest in low-emission alternative transport for short commutes. There are various considerations that we have identified as next steps if the project were to be continued.



## 1. Introduction

America is extremely car dependent in comparison to other nations. Americans drive a car for 85% of their daily commutes, while Europeans make only 50-65% of daily commutes by car. Across the USA and Europe, roughly 30% of commutes are less than one mile, and for these one mile trips Americans drive 70% of the time while Europeans bike, or walk, or use public transport 70% of the time.<sup>1</sup> The overarching mission of this project is to reduce the frequency of short commutes by promoting an alternative transport that is suited for short distances: a convenient electric longboard.

Other forms of alternative transport have addressed the problem of America's car dependency; examples include electric bicycles (e-bikes), mopeds, and car-share programs. To see if electric longboards are a viable alternative transport, this project started with identifying pain points associated with prior solutions. A key disadvantage of e-bikes and mopeds is flexibility. Their size and weight makes it difficult to use as a link between multimodal transportation. E-bikes weigh 38-70 lbs, while electric longboards typically hover around 15lbs.<sup>2</sup> An e-bike is also usually the length of a person while an electric longboard spans around 3 feet and is thin in comparison. Although top-end e-bikes can reach up to a range of 56 miles, 85% of all American commutes are less than 15 miles.<sup>3,4</sup> 60% of commutes are 1-5 miles long, 17% of commutes are 6-10 miles long, and 8% of commutes are 11-15 miles long.<sup>4</sup> In comparison, electric longboards have a range of up to 14 miles. Their element of portability also enables customers to use electric boards as a last-mile solution. If a train station or bus station is a far walk, customers can employ the portability of their board by riding to the station at 15-20 mph and folding up

---

<sup>1</sup> Buehler, Ralph, et al. "9 Reasons the U.S. Ended Up So Much More Car-Dependent Than Europe." *CityLab*, 4 Feb. 2014, [www.citylab.com/transportation/2014/02/9-reasons-us-ended-so-much-more-car-dependent-europe/8226/](http://www.citylab.com/transportation/2014/02/9-reasons-us-ended-so-much-more-car-dependent-europe/8226/).

<sup>2</sup> "Does E-Bike Weight Matter?" *Piccadilly Cycles - Electric Bikes - Ashland - Bicycles*, 12 Mar. 2015, [www.piccadillicycles.com/blog-entries/2015/3/12/does-e-bike-weight-matter](http://www.piccadillicycles.com/blog-entries/2015/3/12/does-e-bike-weight-matter).

<sup>3</sup> Cyclist, Joe. "How to Figure out Electric Bike Range." *Electric Bikes Blog*, 15 Jan. 2016, [electricbikeblog.com/how-to-figure-out-electric-bike-range/](http://electricbikeblog.com/how-to-figure-out-electric-bike-range/).

<sup>4</sup> National Household Travel Survey, Federal Highway Administration (FHWA), <https://nhts.ornl.gov/vehicle-trips>

their board once they arrive.<sup>5</sup> Thus, electric longboards are an alternative transport in their own right and enable commuters to more easily adopt public transportation.

Although electric longboards have a number of advantages, marketing them to the public remains an issue. After testing out a top brand of electric longboard, The Boosted Board, we identified two main weaknesses: portability and affordability. Electric longboards are more portable than alternatives like e-bikes, but they are still heavy and large. High quality electric longboards also cost upwards of \$1,000. Though affordability is a key barrier, we focused on portability, since cost has as much to do with manufacturing and operation costs as it does with board design.

Additionally, our team designed an accompanying smartphone application for the board, which allows users to check battery life, range, and (if location features are enabled) trip history. Through viewing anonymized trip history of riders, our team is able to gain an understanding of how alternate transport infrastructure is utilized and lobby for protected bike and skateboard lanes. Products such as these are integral to the effort of citizens to reclaim the massive amount of urban public space that has been designated for personal vehicles. The application is designed with the dual objective of serving users now by displaying history and usage information and in the future by securely and anonymously analyzing their usage patterns.

This paper is split into four sections, most containing sub-sections. The first section contains the Technical Design, which details the mechanical and software developments of the product. The second section consists of the societal impact of the project, split into sub-sections concerning environmental and social benefit considerations. The third section contains business and miscellaneous considerations considered important to the project, such as regulatory pathways. The fourth and last section concerns regulations on electric skateboards and how that affected our board's design and intended use. An appendix at the end of the paper is regularly referred to, but only serves to justify and reinforce claims being made, rather than introduce any new ideas.



## 2. Technical Design

### 2.1. Mechanical Engineering Technical Design

#### 2.1.1. Description of Approach

From the beginning of the semester, we determined that the primary goal was to make a portable electric longboard. We brainstormed ideas on how to achieve a portable design and thought of three possible design options to make the longboard compact: a foldable design, telescoping design and rollable design. Since the only portable electric longboard currently available, called Linky, employs both folding and telescoping, we initially decided to tackle the niche rollable design. Another motivation for investigating how to make a rollable board was that it could potentially achieve a smaller volume than folding a board in half. Ultimately, after testing various rollable designs, all of which were non-ideal for various reasons, we pivoted from the rolling concept to a folding design. We determined that difference in the amount of volume rolling saves compared to folding is not worth the added complexity and potentially more

---

<sup>5</sup> Prindle, Drew. "Sick of Walking Everywhere? Here Are the Best Electric Skateboards You Can Buy." *Digital Trends*, Digital Trends, 18 Apr. 2018, [www.digitaltrends.com/cool-tech/best-electric-skateboards/](http://www.digitaltrends.com/cool-tech/best-electric-skateboards/).

awkward shape. The volume of a full board, a rolled board, and a folded board are shown in Figure 1. The final design ultimately incorporated many of the design components explored for the rolling designs, but in a simpler and more stable design.

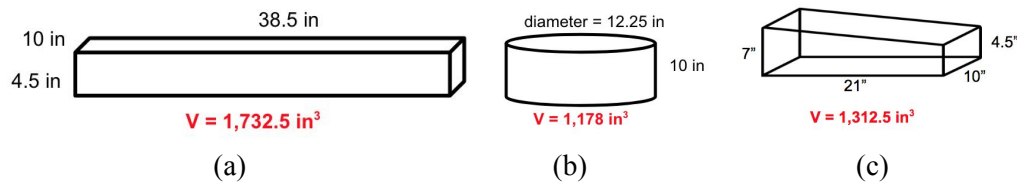


Figure 1: Preliminary calculations of the volume of a (a) full board, (b) rolled board and (c) folded board.

### Panels Connected with Mesh or Hinges

The first connection method we considered was a board made entirely from panels that would be externally connected via a method that constrained rolling to only one direction. Two initial ideas for an external connection were with either an adhesive mesh or hinges. For both ideas, the panels could simply be cut as rectangular pieces in a sheet of wood, making the deck of the board primarily one layer of wood. With the mesh idea, a flexible synthetic material would be glued to the underside of the wood panels. When the board was flat, the sides of the panels would be compressed together, thus keeping the board flat. The board could simply be rolled in the other direction via the flexibility of the mesh. With external hinges, the same flat, rectangular wood panels could be simply attached to each other via hinges. Ideally, the hinges would lock in the flat position, but then be free to rotate when rolling the panels of the board up. We built out a mesh board prototype, but realized several limitations of the mesh design (see image of prototype in Figure 2 below).



Figure 2: First prototype of a rollable design that is comprised of numerous plywood panels connected by ducktape (acting as a temporary mesh) on the underside.

A mesh makes it difficult to control the spacing between the wood panels, thus leading to excessive deflection as shown in Figure 2. Minimizing deflection is key in two ways. The first is that components on the underside such as the battery and controller must be protected from hitting the road, and protection should account for hitting bumps as well. Longboarders desire little to no deflection in the board because ‘flex’ is only possible with no deflection. To have flex in the board means the board has a spring-like quality. Flex makes riding more enjoyable as turning is easier and the board is better able to go over bumpy terrain. Evidently from Figure 2, the mesh design is far from ideal due to its inability to constrain deflection. Thus, it was eliminated as a design option.

### Self-Connecting Hinges

The second connection method we explored was to build hinges into the board. The idea was to 3D print panels that interlock with one another like a hinge. This 3D printable idea has the advantage of making the design modular and open-source. 3D printers are so widely available today that users can 3D print their entire deck themselves. This contributes to the central aim of the project - which is to popularize the alternative transportation that is electric longboards - by making it more accessible to the public.

Similarly, its modularity means that if a piece of the deck breaks, the user can easily 3D print and replace a single panel instead of having to purchase a whole new deck.

We designed and 3D printed numerous self-connecting panels. With each print, we adjusted and iterated the design. Some examples of the prints are shown in Figure 3. The self-connecting panels proved to be aesthetically pleasing and simple. However, they did not lock in place when the board was unrolled flat. Ideally, a deck needs to stay rigid when in its unrolled riding layout to prevent deflecting upwards or downwards when the longboard goes over a bump. It would also be better if the deck is rigid so that the user can easily pick it up and carry it without the deck folding in on itself.

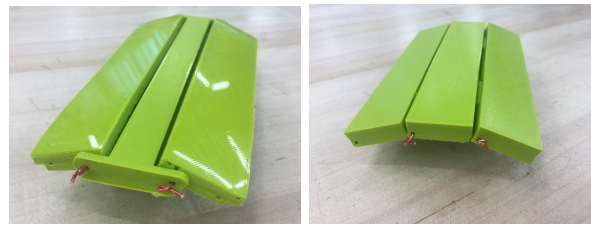


Figure 3: Photographs of 3D printed self-connecting hinge designs.

### Interconnecting Beams

The interconnecting beams design employs the self-connecting panels but includes two series of segmented beams that run through the deck. These beam pieces (slabs) can be shifted to lock the deck into a flat position and also acts as the primary structural support.



Figure 4: Illustration of the interconnecting beam design.

The basic concept behind this idea is to make the board deck rollable when it's not being ridden, allowing users to fold the skateboard and easily carry it around. To achieve this, the board deck should consist of hollow *panels* and *slabs*. All the panels are held in position by hinges. The slabs fit into the hollow spaces in the panels.

At one end of the board, the rider should be able to initiate locking or unlocking depending on their needs. In the locked mode, the slabs are pushed through the hollow panels, each slab spanning over two panels. This way, the panels are joined and the slabs become part of the resultant structure (one long continuous beam) that is rigid enough to bear the weight of the rider. To unlock, the above process is reversed. The slabs are shifted *back* to allow the deck panels to act independently and thus make it possible for them to be rolled around the hinges that connect them.

Structurally, the deck (panels and slabs) has to work as a unit to bear both shear and bending stresses. The hinges connecting the panel only serve a connection purpose. The slabs and panel combination in the locked mode should be able to provide enough strength with limited deflections.

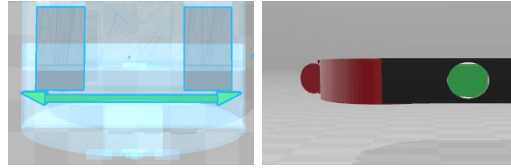


Figure 5: Proposed locking mechanism.

To see the structural feasibility of the design, we conducted a finite element analysis (FEA). An FEA virtually simulates how assembled parts react to forces. It can produce visualizations of the stress distribution and deflection in the assembly.

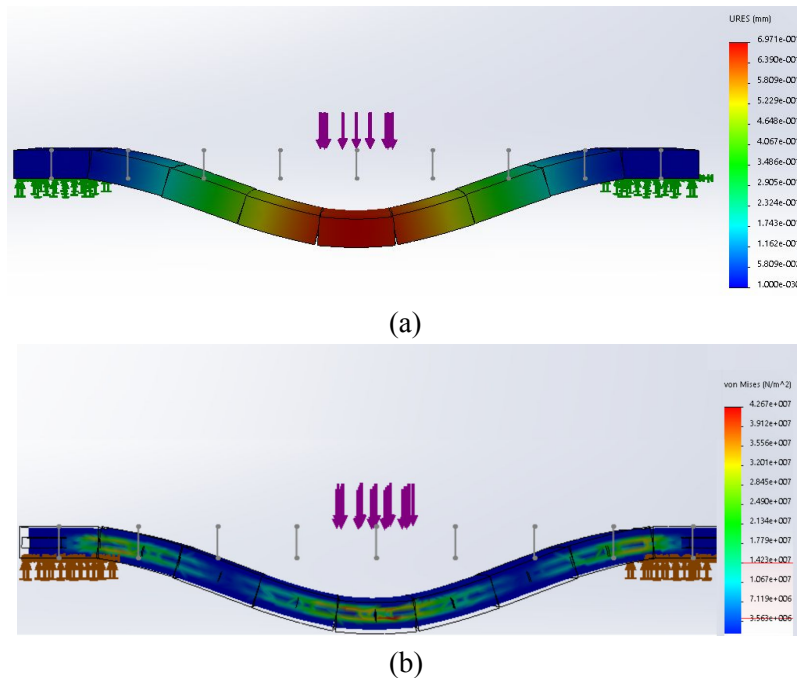


Figure 6: Finite element analysis of the interconnecting beam design. (a) FEA results for the amount of deflection in the board. (b) Sectional view of FEA results for the stress in the board.

The results of the FEA show more stress concentrations on the center of the beam; this part experiences the most bending. The slabs and panels at this section needed to be specially made. Deflection, maximum at the board center, is also displayed as part of the FEA analysis.

The key limitation of this design was the fact that a mechanism is needed to be put in place to ensure that the slabs do not fall out then the board is rolled up for portability purposes. Since the whole concept relies on the ease at which slabs can be moved through the panels to lock or unlock them, the mechanism to ensure that slabs do not fall out is hard implement, and also could make the operation (locking/unlocking) difficult. The many connections between each panel cause the center of the deck to have a substantial amount of cumulative deflection.

Limited by time and scope, we decided not to pursue this concept as our final idea for a rollable skateboard. To minimize deflections (sagging), very thick panels have to be used to take advantage of geometry. The mechanism of ensuring that the slabs do not fall out when the deck is rolled may perhaps be achieved by running a tension cable through each slab. This cable would be attached to the slabs and should connect all of them, and be able to hold them in position (inside the panels) when the deck is rolled.

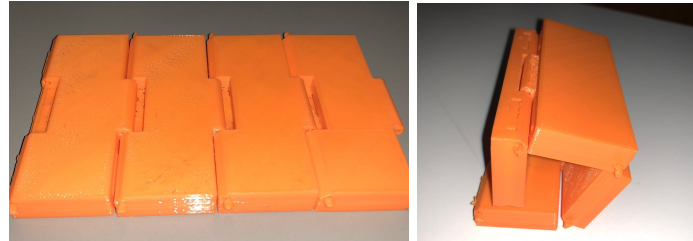


Figure 7: Assembly of 3D printed interconnecting beam prototype

### Ratchet and Pawl Wire Deck

We pivoted to an idea including a ratchet and pawl system in order to introduce a method that would put the board panels into tension to ensure its rigidity when in the flat position. With the earlier idea of self connecting hinges, the board's rigidity was reliant on the geometry of the hinges. Many of the self-connecting hinge designs had very high stress concentrations that could easily result in failure due to the weight of a human. Our idea with the ratchet and pawl system was to make the rigidity of the board instead based on the compression between the panels. A ratchet and pawl system can tighten a cord or strap and lock it in the tightened position. Disengaging the ratchet would allow the cord to be loosened so that the panels could be rolled up. The initial design for this idea was to have wood panels with two wire ropes threaded through the panels to hold them together. The wire ropes would be pinned at one end of the board and would wrap around a pulley at the other end. The pulley would have the ratchet attached to it with a driving pawl and locking pawl (as seen in Figure 8). Rotating the pulley would turn the ratchet and tighten the wire rope, while the pawls would keep the wire rope taut. Drawings of this full deck design are shown in Figure 9.

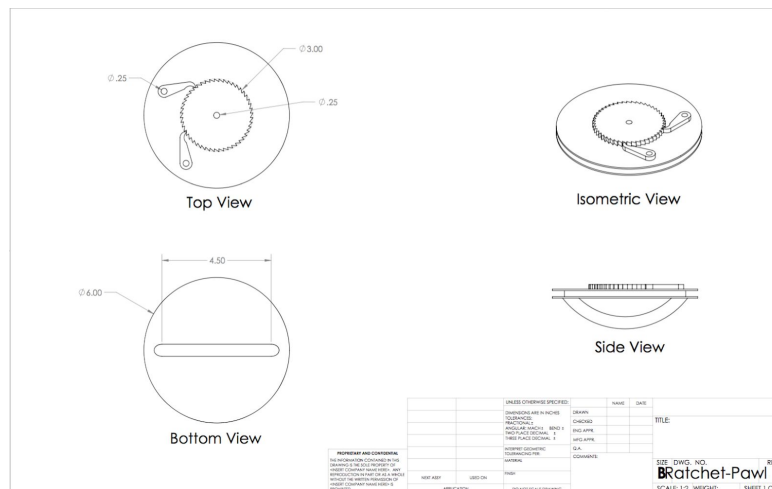
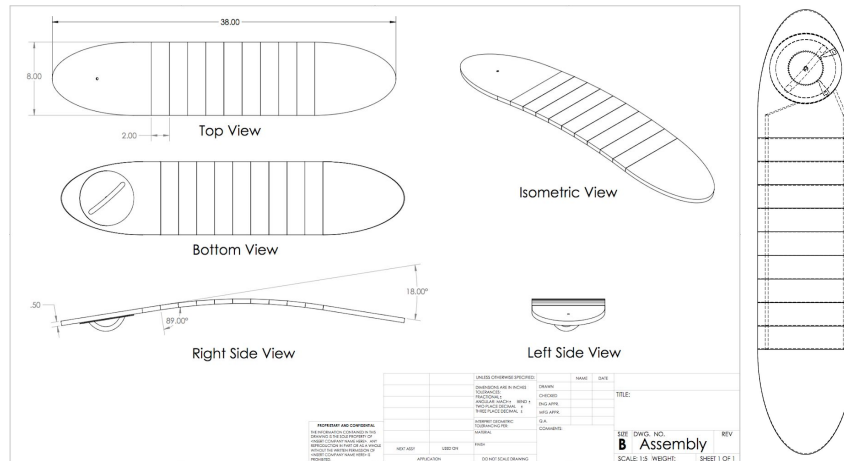


Figure 8: Solidworks drawing of the ratchet-pawl and pulley assembly





To test this idea before building it, we conducted a full stress analysis. All calculations can be found in Appendix 1. This analysis included calculating the tension needed in the wire rope such that the panels would not slip under the load of a human as well as checking for various failure modes. The analysis included failure checks for shear of the wire, excessive tension of the wire, compression and shear of the ratchet teeth, shear of the pin keeping the ends of the wire rope in place, and compressive/tensile force in the wire due to bending. These various checks helped to determine various design constraints. In particular, the calculations showed that there needed to be a high coefficient of friction between the panels, that the ratchet material should be made of steel instead of 3D print plastic, and that the number and thickness of wire rope was very influential in the factor of safety of the system.

Taking into consideration the results of the analysis, we then built out a design with the ratchet and pawl system. Since the calculations showed that a very high tension was required to tighten the wire rope to the point that it would hold the board rigid enough to sustain the weight of a person, we adjusted the ratchet design. Tightening the wire rope to such a high tension would be very difficult to attain via rotating a small pulley by hand. Instead, we purchased a ratchet strap, which is typically used to tie down loads in trucks. These ratchets use a strap instead of a wire rope and are easy to tighten because they users simply crank a handle to tighten the strap and then pull a lever to disengage. For this design, we made the wood panels out of three wood layers glued together to allow for a gap through the panels that the straps to be run through (see Figure 10). The top layer was offset so that there would be an overhang on each panel. This overhang was added to constrain the board to rolling in one direction only. A photograph of the full prototype is shown in Figure 11.



Figure 10: Photograph of the construction of a wood panel.





Figure 11: Photograph of the full ratchet design prototype.

Overall, this prototype did not work well. The design required a very high tension in the straps and it was very difficult to make perfectly aligned panels. The slight misalignment of panels paired with the extremely high tension in the strap required to hold the panels together, we ultimately decided the design was not stable enough nor was it user friendly.

### Final Concept: Self-Connecting Hinges and Structural Rod

After realizing that all of the rolling concept designs were either flawed or too complex to execute successfully (within the given time period), we shifted to designing a foldable deck. The rolling concept required the deck to be made of several panels, which introduces many points of potential failure. We determined the minimum number of panels needed to be able to fold the board while accounting for the placement of the battery, electrical control components, wheels, motor, and trucks. The design components for the folding design were partly inspired by some of the concepts researched for the rolling design. The self-connecting hinges explored earlier worked well, however they lacked a mechanism to keep the board rigid and sturdy when a load is applied. Thus, we introduced structural rods to the design as a method for keeping the board rigid and to take the majority of the load of a rider. The hinges were designed with a slot for rods to be inserted such that the rods would be held directly under the wood panels in the lengthwise direction. A locking mechanism was also designed so the rods could be held in place in two positions. When folding the board, the rods would sit on one panel and stay in position via the locking mechanism (as shown in Figure 12.b); when the board is ready to ride, the rods would be inserted into the hinges and stay in place via the compression of the hinges against the rods and wood panels caused by the pretension in the bolts (as shown in Figure 13.b). The full final design of the board can be seen in Figure 14.

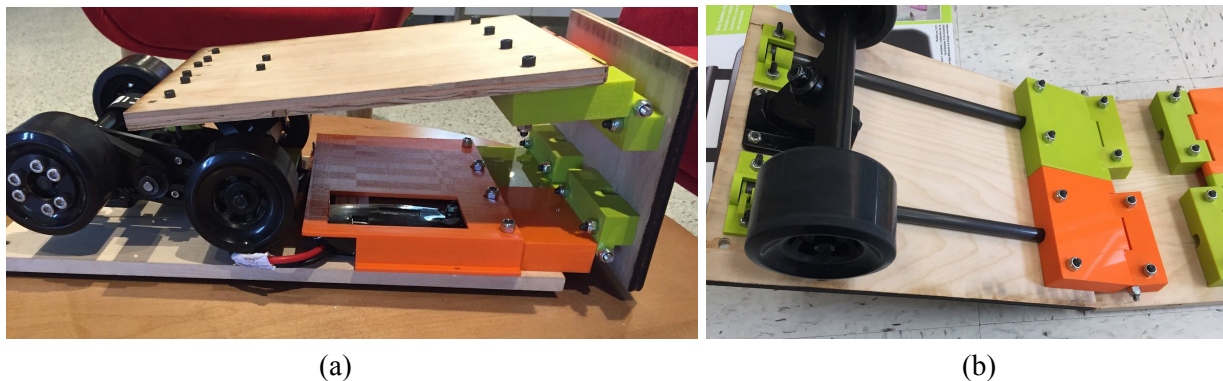


Figure 12: (a) The board in the folded position, (b) View of the structural rod and locking mechanism when board can be folded.



Figure 13: (a) The board in the flat and ready-to-ride position, (b) Underside view showing the structural rods in position.



Figure 14: Full deck design

### 2.1.2. Final Design Drawings

The final design drawings are included in Appendix 2. Below is a view of the exploded assembly of the final design. The final design drawings exclude the mechanical kit (trucks, wheels, drivetrain etc.) as explanations of how to assemble the mechanical kit are readily available online are typically specific to the brand of the mechanical kit bought.

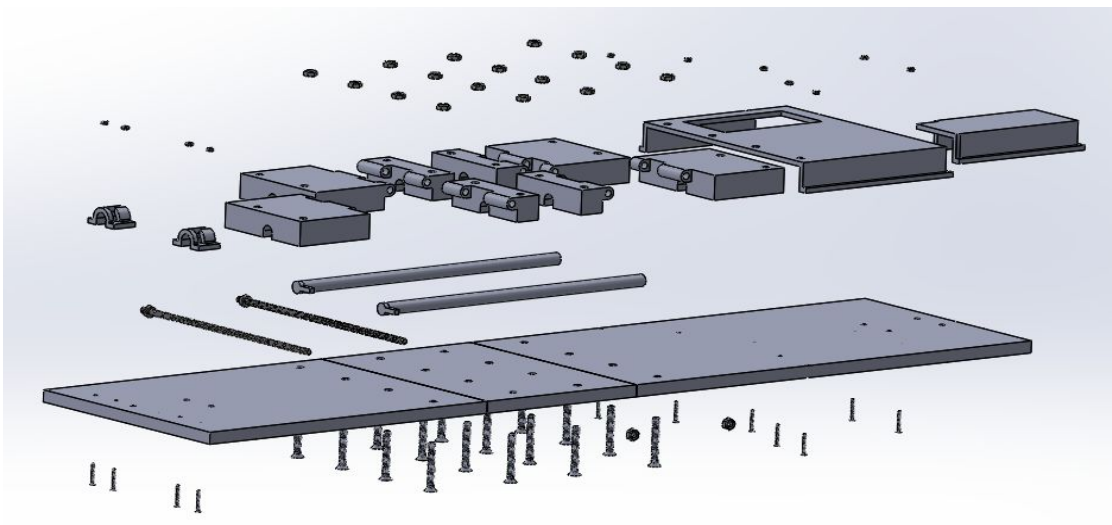


Figure 15: Exploded assembly view of final design.

### 2.1.3. Analysis

#### **Stress Analysis**

We did a series of various stress calculations by hand as well as FEA analysis. All calculations can be seen in Appendix 3. The following calculations were completed: shear of structural rods, bending of structural rods, compression of PLA under bolt pretension, compression of PLA under structural rods, and fatigue of structural rods. The analysis assumes a worst-case scenario load of 250 lbs applied as a point force on the direct center of the board. The average male weight in America is 195 lbs, and with a very heavy backpack of 45 lbs, the total load would be 250 lbs. Various components were sized or some materials were chosen based on achieving satisfactory factors of safety from these calculations. Based on the final design choices, the factors of safety for these various parameters range from 2.5 to 46.5. The fatigue analysis on the carbon fiber rods suggests that they could sustain 500 million load cycles. Assuming a user rides the board twice daily, with four load cycles per ride, the fatigue life would be equivalent to approximately 171,000 years.

#### **Material Selection**

Based on the stress analysis, we identified some material changes that were necessary. First, that analysis suggests that ¼" diameter stainless steel rods that were initially used were not strong enough and would plastically deform under the maximum load of 250 lbs. We researched higher strength materials and ultimately chose carbon fiber rods of ½" diameter. These carbon fiber rods gave satisfactory factors of safety for bending stress, shear stress, and fatigue failure.

The FEA analysis also gave useful results in terms of determining the infill density needed for the PLA hinge. The FEA analysis allowed us to find the maximum stress in the hinge. In the analysis, the hinge material was set as PLA plastic, which in the program runs as a solid piece of 100% infill PLA. With this setting, the hinges were strong enough and would not fail under the application of the maximum load. However, for the actual prototype, the hinges were 3D printed with PLA plastic using an infill of 7%.

We then conducted research regarding strength properties of PLA as a function of infill percentage. Using the maximum von mises stress in the hinge from the FEA in stress analysis calculations, we compared the factor of safety for a print of 90% infill versus 100% infill (see Appendix 3.1). The strength of 90% infill would suffice without severely impacting the quality of the print like 100% infill would. Even if 100% infill density was pursued, it should be printed with an extrusion layer height of 0.2 mm, which would take 28 hours to print a single hinge (4 large hinges are needed). In contrast, to produce the same quality print with an infill of 90% instead, a larger layer height of 0.25 mm can be used, which would cut down print time to 11 hours. Thus, printing with 90% infill and a layer height of 0.25 mm was chosen for the final design.<sup>6</sup>

In addition, the prototype was constructed with two plywood panels and one maple panel. The maple panel had much less splitting at the bolt holes and the analysis was all done only maple. Thus, the deck should ideally be built with all maple panels.

---

<sup>6</sup> Time calculations were done by slicing the prints with the specified infill density and layer height in Duke University's 3DPrinterOS site.

## 2.2. Software & Electrical Engineering Technical Design

### 2.2.1. Electrical Engineering Technical Design

The goal of the electrical hardware in this system is simple: allow the rider to use a remote to control the motor to move the board forward and brake. There are several key components that are used to create this functionality. There is a very established hobby community and vendor ecosystem that has allowed us to purchase most of these parts pre-built and instead focus on unique value-add through our iOS application rather than having to focus on the electrical engineering of the hardware. Considering this, the description of our engineering system will be a more high level view of functionality rather than a detailed elaboration on the electrical engineering at its core.

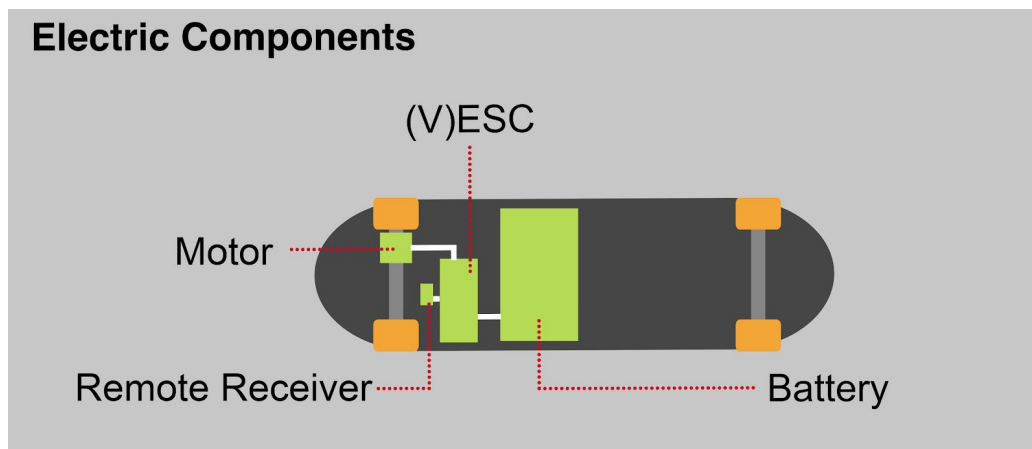


Figure 16: This diagram shows a simplified connection model of the electrical design. Each components' role is explained in detail below.

#### Battery

A 6S2P lithium-ion battery powers the board. The 6S refers to the number of 3.7 volt cells that are placed in series(6), while the 2P refers to the number of parallel series (S) there are (6). For example, in this case, the battery has 2 sets of 6 cells in in series for a total of 12 total cells. In general, placing more cells in series increases your voltage output, which impacts ability to accelerate and reach high speeds (and range to some degree), while placing cells in parallel increases available current, which impacts battery range.<sup>7</sup> Sizing up through different combinations of series and parallel can increase range, torque, or top speed depending on the configuration you choose. The performance measurements for this board are based on a 6S2P battery size, but a full production model will include a larger 10S4P or 12S4P battery, which will greatly increase both the top speed and range. These battery sizings are more typical for production-grade electric longboards.

The [battery we purchased](#) has an integrated charging system, battery management system, and battery percentage display. A potential for cost reduction in future iterations could come in hand-crafting the battery rather than buying a prefabricated battery at a markup.

---

<sup>7</sup> "BU-302: Series and Parallel Battery Configurations." *Serial and Parallel Battery Configurations and Information*, Battery University, [batteryuniversity.com/learn/article/serial\\_and\\_parallel\\_battery\\_configurations/subscribe\\_thx](http://batteryuniversity.com/learn/article/serial_and_parallel_battery_configurations/subscribe_thx).

## Electronic Speed Controller (ESC or VESC)

The electronic speed controller (ESC) is the brains of the board. The ESC is responsible for reading in radio signals for the remote control and routing power from the battery to the motor to control board movement. ESC's are ubiquitous in remote controlled cars and planes, but have also been specially adopted by the electric longboard community. A particular open source ESC that is tailored to electric longboard usage is the VESC. The VESC is the ESC we have used in this board. The VESC provides much more functionality than a basic ESC. It controls and monitors voltage and discharge from the battery to create smooth starts and stops, it has out of the box regenerative braking built in, and has a software package that allows for easy user modification of the ESC's settings. Generally, the VESC is greatly advantageous over regular ESC's because of its added safety in smooth riding, as well as battery voltage control and management. The VESC is sold by [electric longboard hobby websites](#), and has a well-maintained and active development community. It works out of the box, meaning that it really is as simple as connecting to the battery, motor, and remote receiver in order to start using the board.

## Motor

The motor used on this board is a 190KV brushless DC motor. We purchased two motors from an [electric longboard hobby supplier](#), but only used one in our final design. Most production electric longboards have a dual motor setup, but this requires two ESC's. Given that the ESC is a rather expensive component and that this board is a proof of concept rather than a final model, we chose to only use one motor in this design. Future iterations will include a dual-motor setup to increase acceleration and hill-climbing ability.

## Remote and Radio Receiver

This technology uses the same communication methods that are present in all remote control toy cars and airplanes. The remote uses a 2.4 GHz remote signal to communicate with the receiver, which is then translated by the ESC in to electrical signals that drive the motor. The remote can be purchased premade from hobby suppliers and it comes with a receiver. The receiver easily hooks in to the VESC board and requires no setup.

## A Note on Bluetooth

We purchased an [Adafruit Bluetooth LE UART Friend Module](#) to give the VESC Bluetooth capability to communicate with the iOS app, but it is not included in our final design. This simple module, built from an Arduino, can be purchased online and provides convenient software to communicate the VESC data over Bluetooth. The module connects easily to the VESC through the UART port, and the VESC has built in functionality to recognize a Bluetooth connection, so no code needs to be added to the VESC to ensure that the motor and battery data is sent out.

We were successful in testing the use of this module with other electric skateboard apps in the Apple App Store, and we were able to make data transmissions between the VESC and those apps. The pairing between our iOS app and the bluetooth receiver is a goal for future iterations of the board. Given that this component's functionality with our iOS app is still in development, the receiver is not included on the final physical prototype of our board.

## 2.2.2. Software Technical Design

### **Overall Software Design Questions/Purposes**

Many modern electric skateboards such as Boosted<sup>8</sup> and LOU Board<sup>9</sup> offer accompanying mobile applications that allow users to view important board information and trip history, adjust settings, and access product/software update information. We decided to supplement the skateboard with a similar mobile application with two primary objectives in mind:

- **User:** Providing users a key set of features through a mobile application (without requiring its use) enhances the riding experience.
- **Research:** Collecting anonymized data about users' riding and usage behavior would allow us to analyze traffic flow patterns, both to improve our product and to lobby local elected officials and public institutions to improve alternative transportation infrastructure.

### **User Side: Front End App Design**

To best assist users in achieving a personalized riding experience, we provide an iOS application that presents the user's skateboard riding and status behavior in a clean, visual manner. The iOS application is composed of three main components with nine screens:

- **Login:** Control the user's login and registration.
  - **Login - Home:** When the user is not logged in, the home page prompts the user to either register a new account or login into their existing account. Without an account, a user would not be able to use the rest of the application's ride tracking and trip summary features.
  - **Login - Register:** The page contains a main text input section that allows users to input username and password to register a new account.
  - **Login - Login:** The page contains a main text input section that allows users to input username and password to login into their existing account.
- **Ride:** This is where users can check their current riding and skateboard status.
  - **Ride - Home:** This page contains a map view that picks up users' current location, and has a large button to prompt trip start when pressed.
  - **Ride - Riding:** When riding, the application will continue picking up the users' live GPS location, as well as other riding metrics such as speed and duration. Using these raw metrics, we can show users live statuses of their current trip through the application, including other calculated metrics such as distance, calories burned, and CO2 emissions saved.
  - **Ride - Ride Complete:** At the end of each ride, our screen will display the summary trip statistics, as well as a map preview of the completed trip route. The trip information will be saved to the user's history database.
- **History:** This is where users can view information about their past trips.
  - **History - Home:** The home screen of the user profile displays the user's summary trip statistics, such as total trips taken and distance travelled.
  - **History - Ride History:** The ride history screen contains a list of all the user's past trips, sorted and labeled in reverse chronological order. The user can select a specific trip to view individual trip details.

---

<sup>8</sup> Boosted Boards. (2018). Retrieved from [boostedboards.com/](https://boostedboards.com/)

<sup>9</sup> Lou Boards. (2018) Retrieved from [www.louboard.com/faq/](https://www.louboard.com/faq/)



- History - Ride Details: Within each individual trip history page, our screen will display the summary trip statistics, as well as a map preview of the completed trip route. These trip history pages like the ride - ride complete pages, except it will be pulling past trip data from the application database.

This set of features was determined based on analysis of mobile applications of similar products and motivated by the carbon-saving element of this product. The application design skeleton is shown in the image below, which displays the overall user interface storyboard, with the three main components and nine screens as described above:

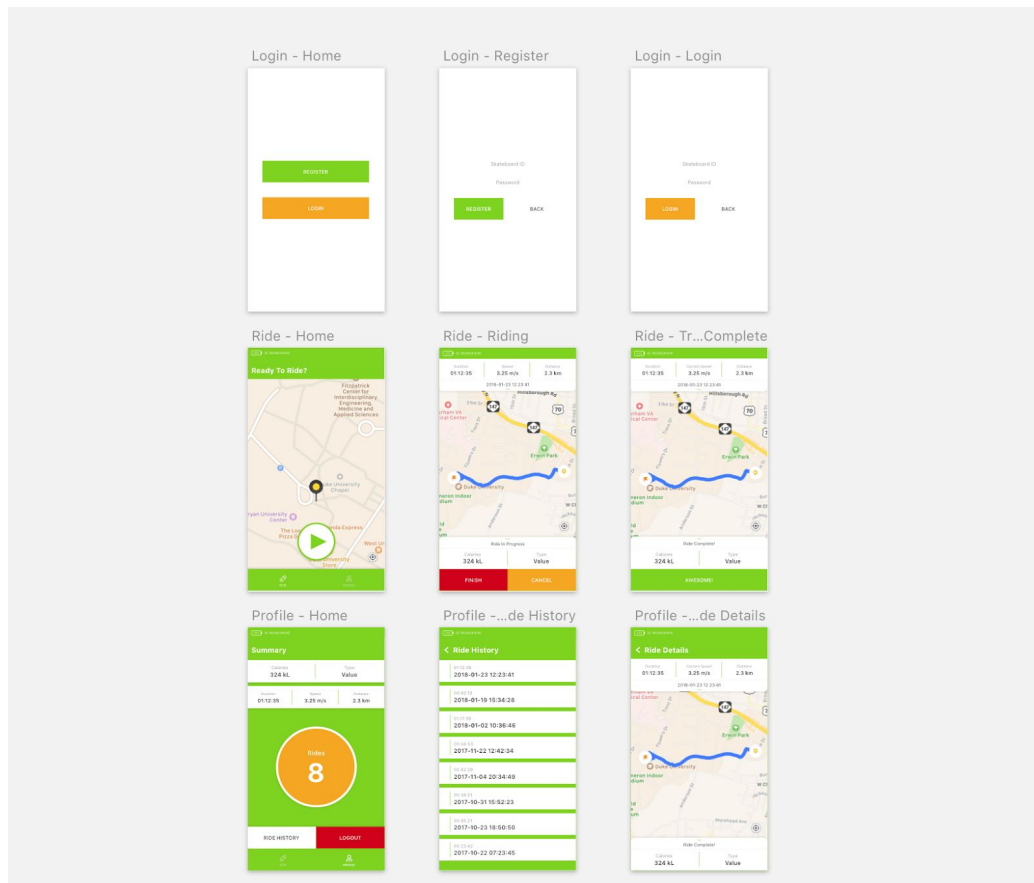


Figure 17: Skateboard iOS Application Design Storyboard.

Within the application, we included a variety of trip statistics that are useful for providing users with trip insights. Specifically, we can break these features down into three categories:

- *Raw, ride features*: These features can be collected and generated directly from phone's system, and are helpful for tracking user riding behavior. These features includes: **GPS Location, Current speed, Map.**
- *Calculated, ride features*: These features are calculated from other raw, ride features, or are created manually within our code, and are also helpful for tracking user riding behavior. These features include: **Ride Duration, Distance Travelled.**
- *Calculated, health/environmental features*: These calculated features are derived from other ride features, and specifically help users understand their trips' environmental and health benefits. We



hope that users will feel encouraged to ride their skateboard more upon seeing these health and environment related statistics. These features include: **Calories Burned, CO2 Emissions Saved.**

## Backend Data Storage Design

To provide users with the insights and features listed in the front end design section, it is necessary to store and retrieve their information. Whenever history metrics are displayed on the screen, the application retrieves previously stored trip information, and whenever a new ride is taking place, the application stores this new trip. In some cases, the application is dynamically updating fields; that is, it is displaying a real-time value that changes and must be updated on the fly, such as riding speed and riding distance during a ride.

Accommodating these tasks requires designing a realtime database that is a flexible and supports these different demands. The Firebase realtime database management system satisfies these requirements, and provides an API (Application Programming Interface) that allows us to connect our application, written in Swift, to the database. Before delving into the structure of the database, it is important to understand the basics of designing a database schema. In Firebase, all data are stored in a JSON (JavaScript Object Notation) format, which is a file-format that transmits data using key-value pairs. A key is one short piece of text that maps to further information. For example, for a specific board the key “Model” may map to “1.0,” which would inform the application that this is the first-generation version of our electric skateboard. Within the key-value model there can be nested keys. A user’s unique ID is a key that is used to map to the start time of each of their trips, but these start times are themselves keys that map to more information about this specific trip. Using this structure, we establish a structure for organizing data about boards, users, and their trips, including location history.

There are three top-level categories storing all of our data: Boards, Trips and Users. Each is a key that maps to more information. At its particular level of storage, keys must be unique. For example, within the Trips section, there cannot be multiple keys with the same name, because these keys represent users within this Trips section. If a customer with the unique identifier “hDbb8Kir6jhOxPZ0EGFmdzSCYg03” takes three trips on her board, all three of these trips should be stored under this customer identifier. However, values don’t have to be unique; if a user takes two trips that are 57 seconds long, the database is fine with this duplication because this field is not a key and does not map to more information.

In the Boards section, every (hypothetical) board has an associated model value and serial number, and users must register a valid serial number to create an account and access the app. When they register this serial number, a new entry is created in Users section. Here, user IDs, which are automatically generated and handled through the built-in Authentication section of Firebase, are associated with skateboard serial numbers. Future generations of boards may ride differently or offer different features, so linking users with the model of their board allows us to customize the app experience and offer users the correct settings for their model of board.

The Trips section of the database stores a new record for each trip a user takes, and these trips are nested under the user’s unique ID. Since the date and start time of the ride are the key, under which the rest of the ride information is stored, we can be sure that this key won’t be duplicated, as it is impossible for one user to start multiple trips at the exact same time. Under this key is stored the duration of the trip, the distance covered, and a latitude and longitude value captured every second during the entire course of the trip.

A closer look at the database structure is shown below:

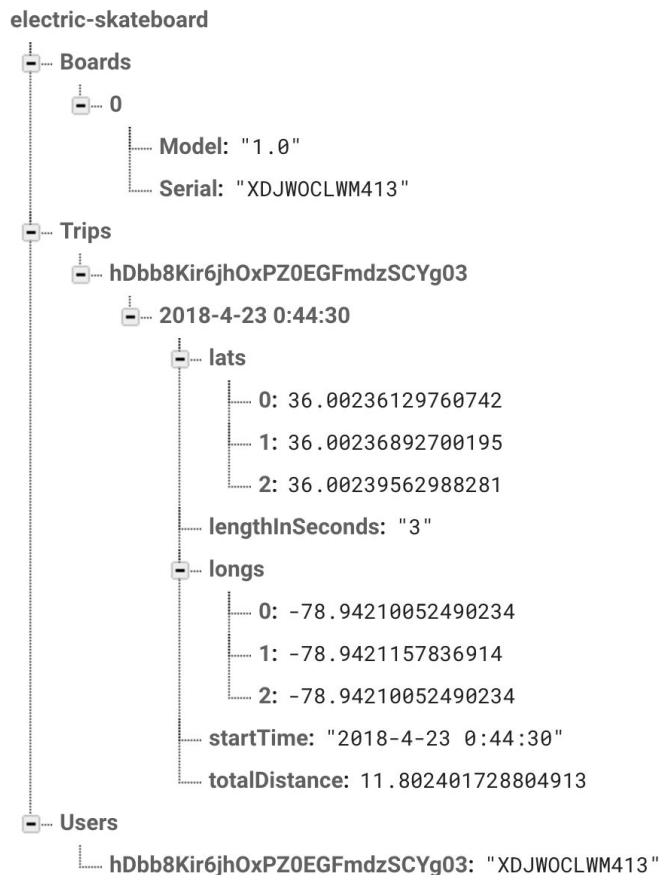


Figure 18: Firebase database structure

This structure allows the application to store new trips and retrieve information about old and current trips. These are the only raw data fields required to serve more complex pieces of information on the front end of the application. For example, aggregate distance is calculated by adding the discrete distances between every GPS coordinate, which allows us to update distance as the rider is taking a trip. Since Firebase supports realtime operations, the application is able to access this information about global positions virtually immediately after they are stored. Other useful metrics such as calories and carbon saved are calculated based on statistics from the EPA<sup>10</sup> and Harvard Medical Center<sup>11</sup>.

## Technical Components

This iOS application was designed in Swift<sup>12</sup> using a combination of the developer applications Sketch<sup>13</sup>, Supernova Studio<sup>14</sup> and Xcode<sup>15</sup>. Data are stored in the back end using Firebase<sup>16</sup>. Recreating the full

<sup>10</sup> Environmental Protection Agency. (2018). "Greenhouse Gas Emissions from a Typical Passenger Vehicle."

<sup>11</sup> Harvard Health. (2018). "Calories burned in 30 minutes for people of three different weights - Harvard Health."

<sup>12</sup> Swift. (2018). Retrieved from [developer.apple.com/swift/](https://developer.apple.com/swift/)

<sup>13</sup> Sketch. (2018). Retrieved from [www.sketchapp.com/](https://www.sketchapp.com/)

<sup>14</sup> Supernova Studio. (2018). Retrieved from [supernova.studio/](https://supernova.studio/)

<sup>15</sup> Xcode. (2018). Retrieved from [developer.apple.com/xcode/](https://developer.apple.com/xcode/)

<sup>16</sup> Firebase. (2018). Retrieved from [firebase.google.com/](https://firebase.google.com/)

application functionality requires an Apple Developer License but all code is available by request and our application is fully-functioning (that is, none of its components are mocked, and real location data are sent from the device to the database).

## 2.3. Testing

We ran several tests with the final prototype to determine its specifications. Testing was done with a rider of the average worldwide weight of 137 lbs.<sup>17</sup> The full prototype weighs about 20 lbs, which is only 5 lbs heavier than the leading competitor in the electric longboard market.<sup>18</sup> The weight of the prototype could also be reduced by making the hinges smaller and by making the board shorter and thinner. When folded, the total volume of the board is 1312.5 in<sup>2</sup> and it spans 20 inches. When unfolded, the board is 38.5 inches long. The deflection of the board at midpoint is 0.125 inches at rest. With 137 lbs applied at the center, the board deflects 1.775 inches. The top speed of the board is 15.2 mph, and the acceleration is 1.23 mph/s, which is equal to 0.548 m/s<sup>2</sup>. Finally, the energy usage of the battery is 22.2 Wh/mile, which means a total mile range of 3.88 miles with speeds of 6-11 mph. As discussed in the Battery section of Electrical Technical Design, the battery used for this prototype was less powerful than would ideally be used. With additional cells added in parallel, increased current should increase the mile range of the board. This should be explored in future iteration of the design.

No typical industry software testing (eg. integration or system testing) was conducted on our code, as this was outside the scope of this project. However, we conducted basic performance tests on the application by employing it in its intended use and verifying output. This was mainly achieved by walking/running between two points and verifying that the application correctly saved the distance, speed, time, and route of this trip in the database.

## 2.4. Technical Design Conclusion

Software, hardware, and electrical designs all underwent major revisions and iteration throughout the semester, but this iteration still represents only the first version of the final product. This prototype board is a proof of concept that shows that it is possible to build a high quality, inexpensive collapsible electric longboard. The technical work done shows that this board is a viable concept that would add value to the market, however there are still routes for improvement which will be discussed in the conclusion. The report from here on out will focus on what the impacts of this board may have if it were adopted and the business plan for eventual release.



## 3. Societal Impact

For urban and suburban commuters, our product provides a practical mode of transport due to convenience afforded by the portable design. Since there is flexibility in how a user might choose to use the product, two primary use cases will be used throughout the Societal Impact section. Case 1 consists of

---

<sup>17</sup> Walpole, Sarah Catherine, et al. "The Weight of Nations: an Estimation of Adult Human Biomass." *BMC Public Health*, vol. 12, no. 1, 2012, doi:10.1186/1471-2458-12-439.

<sup>18</sup> Constine, Josh. "Boosted's v2 Electric Skateboards Go 12 Miles with Swappable Batteries." *TechCrunch*, TechCrunch, 1 May 2016, [techcrunch.com/2016/05/19/boosteds-v2-electric-skateboards-go-12-miles-with-swappable-batteries/](http://techcrunch.com/2016/05/19/boosteds-v2-electric-skateboards-go-12-miles-with-swappable-batteries/).

the electric longboard product being used as the primary transportation vehicle toward a destination. This scenario is realistic for shorter commutes of five miles or less. For projections of societal impact using Case 1, it is considered that two percent of individuals who currently use a light duty vehicle (LDV) to commute would become users of the electric longboard. Case 2 consists of the electric longboard being used as a “last-mile” solution toward a public transportation station. In this scenario, the user can be seen as someone who commutes via LDV to also access public transport stations. This individual might also be subject to a longer commute than the individual from Case 1, where the use of public transport might be necessary due to the limited range of the electric longboard. For projections of societal impact using Case 2, it is similarly considered that two percent of individuals who currently use a LDV to commute would become electric longboard users. These users may be inclined to doing so because the convenient portability of the electric longboard makes the use of public transport more feasible.

### **3.1. Environmental Benefit Analysis**

#### **3.1.1. Carbon Emissions**

To quantify the carbon savings of using electric longboards as an alternative to cars, we calculated the amount of carbon dioxide equivalent emitted by a car over 4 miles (the mile-range of the prototype) versus an electric longboard (see Appendix 4.1 for the calculations). The calculations estimated that a gasoline fueled car would produce 1.53 kg of carbon dioxide equivalent over the 13 miles. An electric longboard, on the other hand, would emit 0.042 kg of carbon dioxide equivalent. This is equivalent to 2.8% of the carbon emissions of the gas car. Evidently, mass adoption of electric longboards to replace short car commutes would have significant carbon savings.

The calculations assume that the electric longboard is fully charged by electricity produced from methane power plant. Depending on the state the electric longboard is used, this can overestimate or underestimate the carbon emissions produced by the electric longboard. For example, in California, renewables, large hydro and nuclear accounted for 27.9%, 12.3% and 9.6% respectively of the state’s electricity generation in 2016, while natural gas supplied 49.9% and coal supplied 0.16%.<sup>19</sup> In Florida, on the other hand, coal supplied 23% of the electricity generated in 2014 and natural gas supplied 61%. Renewables, hydro and nuclear supplied the remaining 16%.<sup>20</sup> In the case of California, the carbon emissions of a longboard would be almost halves as 49.8% of electricity comes from carbon-free sources. In Florida, a quarter of electricity generation coming from coal would raise the carbon emissions of the electric longboard. After all, comparing a new methane-based power plant to a new coal power plant, natural gas emits 50-60% less carbon dioxide than coal.<sup>21</sup> However, when recalculating the carbon savings of the electric longboard using Florida’s fuel mix, the carbon dioxide emitted per mile increased from 0.0105 kg<sub>CO2</sub>/mile to 0.0105105 kg<sub>CO2</sub>/mile. Evidently, even when taking into account the contribution of coal to the fuel mix, the 0.105 kg<sub>CO2</sub>/mile is a fair and fairly conservative estimate of the carbon emitted by the electric longboard. Thus, regardless of state, the electric longboard will save significantly more carbon than a gasoline car.

---

<sup>19</sup> Nyberg, Michael. “Total System Electric Generation.” *California Energy Commission*, 23 June 2017, [www.energy.ca.gov/almanac/electricity\\_data/total\\_system\\_power.html](http://www.energy.ca.gov/almanac/electricity_data/total_system_power.html).

<sup>20</sup> “Florida Energy Facts.” *Florida Energy Facts - FESC*, [floridaenergy.ufl.edu/florida-energy-facts/](http://floridaenergy.ufl.edu/florida-energy-facts/).

<sup>21</sup> “Environmental Impacts of Natural Gas.” *Union of Concerned Scientists*, [www.ucsusa.org/clean-energy/coal-and-other-fossil-fuels/environmental-impacts-of-natural-gas#.WueTb9PwbFY](http://www.ucsusa.org/clean-energy/coal-and-other-fossil-fuels/environmental-impacts-of-natural-gas#.WueTb9PwbFY).

To see how much carbon would be saved if the electric longboard was widely adopted, we calculated how much carbon would be saved if:

- **Case 1:** 2% of light duty vehicle (LDV) commuters who take trips no greater than five miles long adopted the electric longboard. It is predicted that the annual light duty vehicle (LDV) carbon emissions in the United States would be cut by 1.17% (12,431,491 tonnes of CO<sub>2</sub>/year). The derivation of this prediction can be found in Appendix 4.2. This scenario is a viable consideration since data from the National Household Travel Survey in Appendix 4.3. shows that around sixty percent of light duty vehicle commutes are under five miles in length.<sup>22</sup>
- **Case 2:** 2% of LDV commuters in a metropolitan area used our product as a “last-mile” solution enabling public transportation based commutes, our calculations suggest that carbon emissions from the *overall* transportation energy mix (in the metropolitan area) will be reduced by at least 1.14%. Appendix 4.4 shows how this prediction was derived. Unlike Case 1, Case 2 was assessed using a sample metropolitan city, since public transportation infrastructure is not uniformly accessible in many suburban areas.

### 3.1.2. Material Choices

We focused on choosing materials and components that would have minimal environmental impact. Table 1. shows the materials we used for the final design.

| Material       | Environmental Impact   |
|----------------|--|
| PLA Plastic    | Biodegradable (made from fermented plant starch)   |
| Carbon Fiber   | Long lifecycle, recyclable, energy intensive to produce (more so than steel)                       |
| Maple          | Often grown/harvested sustainably, native to U.S.  |
| Steel          | Production is energy intensive and emits GHG (not as much as Al and other metals), recyclable.     |
| Li-ion Battery | Very long life, can be recycled, contributes to resource depletion of cobalt, copper, nickel, etc. |

Table 1: Summary of the environmental impacts of key materials used in the final design.

## 3.2. Social Benefit Analysis

As a result of replacing inefficient single-occupancy LDV travel, the portable electric longboard is afforded favorable social benefits that justify its adoption. Due to the diversity of the social benefits, it will be helpful to organize them into economic and health categories. Environmental considerations on social benefit are also discussed in this section. These motivating factors will each be assessed for benefits and possible disadvantages of our product’s adoption. If the electric longboard is adopted by commuters, this section ultimately finds that the social impact would be overwhelmingly positive.

The previous section detailing the environmental benefits of the electric longboard discusses two scenarios: Case 1 and Case 2. Each considers different ways that the product might be adopted by

---

<sup>22</sup> National Household Travel Survey, Federal Highway Administration (FHWA), <https://nhts.ornl.gov/vehicle-trips>

commuters. While this social benefits section will also consider the two cases, it was not found that either case featured different social outcomes. For the economic and health categories of this section, the benefits are found to be the same for both cases. For both cases, the environmental aspects of the social benefit are promising. With Case 1, the previous environmental benefit analysis shows the carbon savings associated with commuting via an electric longboard that is more efficient than a LDV. Similarly, Case 2 in the previous environmental benefit analysis shows how public transport is a more efficient way to commute than LDV travel.

A “business as usual” baseline marker is proposed here, consisting of the conventional way commuters currently travel. While it is impossible to control for all externalities associated with the our market solution, a reasonable assumption about the adoption of the electric longboard product is made. Like the prior environmental benefit analysis, this assessment proposes that the electric longboard product is adopted by two percent of commuters who would have otherwise resorted to taking a LDV. These commuters are identified as adults who live in urban or suburban areas of the United States. It is also assumed that an increased use of public transport is indeed aligned with reduced commuting times due to reduced car traffic, as suggested by a study from the Texas A&M Transportation Institute, which found that without public transit, USA car drivers would have an additional 785 million hours of delay each year.<sup>23</sup> One example market illustrating this effect is in Boston, where data from 2010 shows that public transport has saved regional drivers nearly 32.9 million hours of road stall. With these reasonable assumptions set, it is now possible to address the social benefits.

Case 1 entails shorter trips of five miles or less, where users would just use the longboard itself as the primary means of transportation. In Case 2, users find the electric longboard appealing because they are offered a new convenience in easier access to public transport stations enabling access to work (Case 2). The impact of *both* Case 1 and Case 2 is a decreased dependence on personal cars, resulting in a smaller number of individuals commuting via car than would otherwise be the case. There are two objections that might be made to counter this claim. Those will be addressed next.

The first objection might argue that our product would not solve traffic congestion. It is true that the number of cars and the level of traffic congestion in the US is rising (see Appendix 4.5). Even if this growth is assumed to continue, however, the adoption of the electric longboard would promote social benefit since it would serve to mitigate that undesirable growth. The second objection that might be made is that some individuals might choose not to abandon their vehicles. Some individuals might choose to share cars with neighbors instead. In this case, some studies have indicated that each shared car takes between 10 and 25 cars off the road.<sup>24</sup> Thus, despite these two possible objections to the claim, it is found that the electric longboard will help mitigate the negative effects of increasing LDV commutes.

Currently, the average commuter wastes 42 hours in traffic every year.<sup>25</sup> Shorter commute times caused by the use of our product in the market means that time is being saved for commuters, impacting the economic, health, and environmental motivations that comprise social benefit. Economically, the time savings from congestion leads to improved productivity. From a social health perspective, the time savings from congestion means commuters face reduced frustration from long commutes. From an

---

<sup>23</sup> Miller, Virginia. 20 Jan 2011 “Public Transportation Relieves Traffic Congestion”

[http://www.apta.com/mediacenter/pressreleases/2011/Pages/112001\\_TTI\\_Report.aspx](http://www.apta.com/mediacenter/pressreleases/2011/Pages/112001_TTI_Report.aspx)

<sup>24</sup> “Carsharing’s Impact on Household Vehicle Holdings: Results from a North American Shared-Use Vehicle Survey.” Retrieved from [https://www.cambridgema.gov/~media/Files/CDD/Transportation/PTDM/PTDM\\_Impact\\_on%20Vehicles.ashx](https://www.cambridgema.gov/~media/Files/CDD/Transportation/PTDM/PTDM_Impact_on%20Vehicles.ashx)

<sup>25</sup> Anderson, Tom. “Commuters waste a full week in traffic each year” 9 Aug 2016.

<https://www.cnn.com/2016/08/09/commuters-waste-a-full-week-in-traffic-each-year.html>

environmental standpoint, the reduction in congestion means that ICE vehicles are spending less time idling in traffic and burning fuel, thus reducing emissions. From the prior section's environmental benefit analysis, it was found that both Case 1 and Case 2 result in reductions in carbon emissions.

### **Economic Benefits:**

Due to the similarities between electric bikes and electric skateboard modes of transport, several social benefits can be borrowed from studies conducted on the impact of increase bike use in society. One such social benefit includes increased economic activity in local communities. The Bicycle Coalition of Greater Philadelphia organized a list of studies that provide evidence to the claim. One such study shows that cyclists spend the most money at local businesses, as depicted by the table below, which uses data from a 2012 study of shoppers in New York City's East Village district.

|                |       |
|----------------|-------|
| Bicyclists     | \$168 |
| Pedestrians    | \$158 |
| Car drivers    | \$143 |
| Public transit | \$111 |

Table 2: Money Spent at Local Businesses Per Capita Per Week by Different User Types <sup>26</sup>

Other studies confirm the trend that bicyclists participate and spend more at local businesses than those who drive. In Seattle, the institution of bike lanes led to a 350 percent increase in sales index two quarters after the installation of bike lanes. In Fort Worth, Texas, the development of bike lanes led to a 179 percent increase in restaurant revenue.<sup>27</sup> This trend is unsurprising; travelling a commute via bike along a route with restaurants along the way offers more convenient access than any car might offer. It is not outrageous to propose that an electric skateboard would afford the same benefits. In the midst of an economic era seeing local business sales drop against an online sales boom, there are compelling arguments that our product could protect local business, or even help fuel a local economic revitalization.

### **Health Benefits:**

In addition to the health benefits discussed earlier due to reduced traffic congestion frustration, additional physical health benefits exist as well. Since our product would enable fewer vehicle miles travelled (VMT) than would otherwise occur, fewer vehicle emissions will pollute urban environments. The impact of this change provides potential benefits to lung health for urban populations, leading to the reduced disease instance, progression, and costs associated with health problems caused or exacerbated by city pollution in the future. Another health benefit for users of our product includes how studies suggest it might help promote more a more healthy body weight. Studies by the American Journal of Preventive Medicine show that subjects who commuted by car on a daily basis gained nearly twice as much weight over a five-year period as those who didn't have a car based commute.<sup>28</sup> Lastly, another social benefit can

<sup>26</sup> "East Village Shoppers Study." *Transalt*, [www.transalt.org/sites/default/files/news/reports/2012/EV\\_Shopper\\_Study.pdf](http://www.transalt.org/sites/default/files/news/reports/2012/EV_Shopper_Study.pdf).

<sup>27</sup> Blue, Elly. "Bikenomics: Bike Lanes on Main Street." *Resilience*, 1 Oct. 2013, [www.resilience.org/stories/2013-10-01/bikenomics-bike-lanes-on-main-street](http://www.resilience.org/stories/2013-10-01/bikenomics-bike-lanes-on-main-street).

<sup>28</sup> "Commuting by Car." Sugiyama, Takemi et al. *American Journal of Preventive Medicine*, Volume 44, Issue 2, 169-173



be attributed to the playful nature of our product. While practical, the mechanism by which the board folds into portable form was designed to be delightful in nature, such that it might promote discussions from new audiences that might later adopt the product.

While it is strongly believed that the social impact of our product will be overwhelmingly positive, there is potential for negative consequences. In 2015, 5376 pedestrians were killed in traffic crashes in the United States.<sup>29</sup> Alarming, pedestrians are 1.5 times more likely than passenger vehicle occupants to be killed in a car crash on each trip.<sup>30</sup> Assuming the same rate of accidents take place with riders of our product, it is safe to assume the increased adoption of our product will lead to a proportional increase in deaths due to electric skateboard and longboard transport. However, cities can take steps to mitigate this impact. For instance, the development of bike lanes along roads can similarly protect and promote safety for users of our own product, since users can travel along such lanes. Moreover, some studies even suggest that such designated lanes in urban areas actually improve traffic flow.<sup>31</sup> This finding suggests that the negative social impacts of our board's adoption are minimal, since criticism of our board on this premise would be akin to suggesting commuters should drive 5 minutes to work rather than walk 5 minutes, just because it is safer to drive than walk. Overall, we believe that the economic, health, and environmental social benefits of our product vastly outweigh its potential negative impacts. Moreover, the acknowledged negative impacts can be mitigated through adequate training and coordination with municipalities, through the development of features in the city such as designated bike lanes.



## 4. Business Plan

This section will analyze the market for the longboard as well as the business plan for the board's production.

### 4.1. Target Market Analysis

The electric longboard has emerged over the past 5 years as a transportation method for mid-range urban commutes<sup>32</sup>. Electric longboards have typically allowed for longer range travel than walking or regular longboarding by using electric power rather than human energy, but they are also more convenient than typical long range travel options, such as public transport and cars, due to their route flexibility and non-need of parking. To top it off, they are simply fun. Longboarding is a recreational sport, and electric longboards allow you to bring recreation to something many people dread in commuting.

---

<sup>29</sup> National Highway Traffic Association. *Traffic Safety Facts*. U.S. Department of Transportation, 2015, [crashstats.nhtsa.dot.gov/Api/Public/ViewPublication/812375](https://crashstats.nhtsa.dot.gov/Api/Public/ViewPublication/812375).

<sup>30</sup> Beck LF, Dellinger AM, O'Neil ME. Motor vehicle crash injury rates by mode of travel, United States: Using exposure-based methods to quantify differences. *Am J Epidemiol* 2007;166:212–218.

<sup>31</sup> Trottenberg, Polly. *Protected Bicycle Lanes in NYC*. New York City Department of Transportation, Sept. 2014, [www.nyc.gov/html/dot/downloads/pdf/2014-09-03-bicycle-path-data-analysis.pdf](http://www.nyc.gov/html/dot/downloads/pdf/2014-09-03-bicycle-path-data-analysis.pdf).

<sup>32</sup> Pierce, David. "The Electric Skateboard Company That Would Take Over the World." *Wired*, Conde Nast, 3 June 2017, [www.wired.com/2016/08/electric-skateboard-company-take-world/](http://www.wired.com/2016/08/electric-skateboard-company-take-world/).

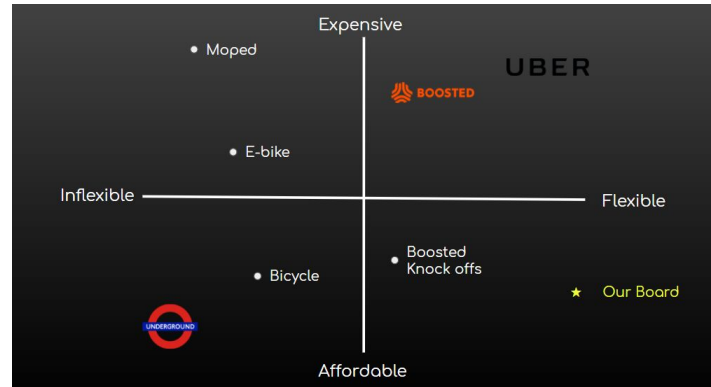


Figure 19: Mapping of existing alternative transports and our electric longboard in terms of flexibility and cost. Modified from in-class Concept Presentation.

While existing electric longboards have helped fill part of this transportation gap, they have not *integrated* long and short transit as they could. Electric longboards, as they are, are heavy and hard to carry. They are hard to walk with if any of your commute cannot be skated. Due to their bulk, they cannot be easily brought into most stores and restaurants, and unlike bicycles they cannot be stored outside due to their risk of theft and lack of locking options. As it is, the electric longboard is very good for a specific type of travel (10-mile round trip commutes with paved roads, bike lanes, and a secure place to store it at your destination), but have been poor at doing much else.

We have built a more portable electric longboard, which allows the board both to fill its unique transportation gap, while also allowing flexibility to integrate with existing transportation infrastructure when needed. This allows for integration into public transport, ride-sharing, driving, or walking if need be. The foldable electric longboard can be both a last-mile tool for a dynamic commute that combines several transportation options, or a mid-range commuter that fits in to changing plans and is flexible for when alternative transportation options needs arise. It improves upon the commute in a same way typical electric longboards do, but without as many drawbacks.

The iOS app additionally helps put the board on equal playing field with other boards on the market with apps, but also allows for hobby riders to gain a deeper level of engagement with their rides through route history and statistics.

We believe there to be a unique market who would be interested in a product with these solutions.

| Geographic   | Demographic  | Behavioral   | Psychographic   |
|--|--|--|---|
| People who have at least some part of their commute with a developed bike lane infrastructure [urban]. | Age: 20-30<br>Socioeconomic:<br>Willing, and able, to spend ~800\$ on board. | Regular use in day to day commute.<br><br>Status gained from having something different or cool. | <i>Green</i> lifestyle<br><i>Liberated</i> lifestyle<br>Travelers.<br>Early adopters/<br>tastemakers.<br>Want to have <i>fun</i> commuting. |

Table 3: Summary of target markets for the collapsible electric skateboard

Given these characteristics, our target user is a: young urbanite looking for a fun, flexible, environmentally friendly, and convenient way to commute. They might be looking for something to do their whole commute with (Case 1 from Social Benefits), but can be easily stowed and transported as they go through their day and encounter new plans. Alternatively, they might be someone looking for a better last-mile solution for their multi-stage commute (Case 2 from Social Benefits). They are interested in trying something new and are comfortable being an early adopter - and are willing to spend to do so.

## 4.2. Moving the Longboard to Market

This board will be released as an “open-source” project, available through this paper publicly and free of charge. Considering that we will probably not be continuing their involvement with the product past this semester, this allows adoption of the board design and concepts without continued involvement. This means we will not need to build out a supply chain or full-scale consumer facing business. All components of our board are open source, and the only barrier to construction is access to the internet to order parts and a basic 3D-printer to build the hinges. The means of moving our product to market will be via distribution our knowledge rather than a packaged product itself. Both our iOS app code as well as the files needed to 3D print board components are open-source. We have done the heavy lifting in terms of stress-testing and proofing the engineering design of the board, but the consumer will be responsible for the final step of building it. The benefit of this option is that our team does not have to actively be involved with continuing development of the board, but users can continue to build the board and realize its benefits. In this sense, we frontload the work, but we do not monetize it. Our work could be considered akin to scientific research: free information for all to use and benefit from, but needing help from others to actualize our research into a product.

We believe this business model not only encourages adoption, but also engagement. The open-source model allows us to avoid the overhead of operational costs, meaning our board is as cheap as the components needed. Our test board comes in well below the roughly \$1500 price point of most current boards on the market. Additionally, users that take the time to work with and build the board become engaged with it - and deeply engaged users become ambassadors for the product.

There is a market specifically for this type of DIY electric longboard. One can easily browse handfuls of forums (like <http://www.electric-skateboard.builders/>), where deeply committed hobbyists discuss their DIY boards, to see that this is true. Users value the control that DIY gives them over prefabricated direct-to-consumer boards, and we believe that our board will fit in well to this customer niche. Additionally, it means that others can take our board design and continue to improve it, free of charge, to ultimately continue building a better product and encourage adoption of this alternative transportation method.

There are downsides to open source in that it is possible that the project does not generate interest from many people and the iteration and adoption that we discuss above does not happen. Additionally, the open source method might alienate users who wish to receive a final pre-built board rather than build their own. Given that we will not be able to continue involvement moving forward, we feel that open-source it is the best option available despite these downsides.

### 4.3. Costs of Production

The full bill of materials for the research and development over the course of the semester is included in Appendix 5 and totaled to \$1,269.35. A bill of materials for the final design is included in Appendix 6 and totaled to \$782.07.



## **5. Other Considerations**

### General Regulations Regarding Electric Longboards

There is a federal law specific to electric skateboards or longboards that sets an age limit of 16 and a speed limit of 35 mph. However, the law states that further regulations are largely left up to the state.

As of now there seems to be no specific laws regarding electric skateboards or longboards in North Carolina. In general however, the NC DMV requires registration of all low-speed vehicles that are to be used on the road. This includes mopeds, which the most similar form of vehicle that has specific laws dictating its use. Since 2015, Mopeds are required to be registered but no driving license is required. Mopeds have a speed limit of 30 mph.

California, on the other hand, has created laws specifically for electrically motorized skateboards. Electrically motorized skateboards cannot have a power system greater than 1000W, and they cannot have a top speed greater than 20 mph. When actually using them on public roads and sidewalks, however, the speed limit is 15 mph.

Figuring out the regulations that apply to electric skateboards is an important to this project for several reasons:

1. Regulations control who the target consumer base is by controlling who is allowed to use electric skateboards. We know from the regulations the people who can use our board has to be above 16 years old.
2. It controls where people use them. Hence, it affects the operating conditions we must design for. Since North Carolina does not recognize electric skateboards as vehicles, they cannot be used on roads as of now, but this will likely change when specific laws like those in California are developed. Thus, we designed for use on both on paved sidewalks and roadways.
3. Finally regulations control the speed restrictions, which is important because top speed is a key parameter in designing the mechanical components. It made sense to design for a top speed of 15 mph, as that is what California's regulations restricts the use of electric longboards to.



## **6. Conclusion**

We were ultimately able to integrate the portable deck design with a user-friendly app to create a full-package product that is ideal for our target market.

In terms of the mechanical design, we designed a longboard deck that folds to save space and makes the board easier to carry. Though all of the rolling design prototypes failed, it was valuable for us to see the

complexities of building out a design that in theory works but in practice does not. By iterating through several different prototypes, we gained a lot of knowledge on various connection mechanisms and structural components. The self-connecting hinge and the interlocking beam ideas explored for the rolling concept both provided a basis for the final design. The hinges were modified to hold structural rods in place. The interlocking beam idea was based on the concept of utilizing a structural beam as the main component to take the load; in the final design, we incorporated a structural beam to add structural integrity and strength to the board. Ultimately, it was critical that we pivoted away from rolling and to folding. With the 3-panel folding design, the board is overall much simpler and more stable, but also saves considerable space. The simplicity of the board also lends well to the business model of a modular, do-it-yourself concept.

To further meet the needs of riders, we have developed an app that creates a link between a rider's mobile phone and their skateboard. The two main purposes of our software iOS application is to enhance users' skateboard riding experiences, and aid transportation research by creating a data collection platform for collecting skateboard usage data.

On the user end, the application mainly enhances riders experiences by providing a visual platform for viewing skateboard and ride information. Again, the software component is not intended to be an essential part of skateboard riding - as this could cause inconvenience, but an enhancement that the user has a choice of implementing in their skateboard riding experience. The iOS application's capability to display information cannot be achieved purely by the mechanical skateboard, and the combination of software and hardware helps make skateboard riding a practical and fun experience for users who choose to implement it.

On the research end, our application serves as a direct platform that links user transportation behavior data to analysts interested in researching alternative transportation usage and trends. The collected data is powerful in that it can inform analysts and researchers of multiple skateboard usage metrics (location, speed, distance) down to the accuracy of one second. The software team also realizes the importance of protecting personal data, especially with information as sensitive as location data. The data collected through our iOS application will be stored securely, and will only be used by researchers with benign intentions.

In terms of next steps, there are some improvements that could be implemented to make this skateboard better, and enable it to further meet the needs of riders.

From a mechanical standpoint, we believe that the overall volume of the skateboard could be reduced to make it more portable. Since portability is a key objective of this project, the need for more iterations to better achieve it will be necessary. Some of the ideas that we suggest for future considerations include careful selection of materials to reduce the overall volume and weight of the skateboard while preserving the structural strength. In addition, the current mile-range of approximately four miles could be increased by carefully selecting a battery of larger capacity, and can still fit into the skateboard without interfering with its mechanical functionality (i.e the board should still be able to fold).

There are also opportunities to improve the mobile application. Cleaning up the user interface and implementing automatic trip start/stop would both enhance the experience. Adding networking features, such as a recent trip history heatmap and showing community statistics, would allow us to leverage user data for research/optimization purposes as alluded to in the software section.

This board represents a first iteration of our concept, and it is part of a larger process of current innovation in the transportation sector. This is a successful first prototype that will hopefully be adapted and developed further to become a viable commuting tool that is a part of the greater disruption of car-based transportation.

## 7. Appendices

### Appendix 1. Ratchet and Pawl Wire Deck Stress Analysis

#### 1. FAILURE CHECK: SHEAR OF WIRE

|  | Amount   | Unit  | Symbol             | Formula  | Source/Notes  |
|--|--|---|--------------------|--|---|
| <b>Forces</b>                          |  |   |                    |  |   |
| Shear Force                            | 1128.15  | N   | F <sub>shear</sub> | 115kg*9.81   |   |
| <b>Wire Parameters</b>                 |  |   |                    |  |   |
| Description:                           | Weather-Resistant Coated Wire Rope-Not for Lifting<br>Ultra-Flexible Galvanized Steel, 1/8" Diameter, 3/16" OD. \$0.68/ft. McMaster-Carr #8912T51. |   |                    |  | <a href="https://www.mcmaster.com/#8912t51/=1bpqmjf">https://www.mcmaster.com/#8912t51/=1bpqmjf</a> |
| Diameter                               | 0.125  | in  |                    |  |   |
|  | 0.00318  | m   | D <sub>w</sub>     |  |   |
| Capacity                               | 400  | lbf   |                    |  |   |
|  | 1779   | N   | F <sub>c</sub>     |  |   |
| Area                                   | 4.68E-06   | m^2   | A <sub>w</sub>     |  | Derated area of wire rope calculated from strand arrangement.                                       |
| Rated Allowed Tensile Stress           | 380  | MPa   | S <sub>c</sub>     |  |   |
| Number of Wires                        | 2  |   | n                  |  |   |
| <b>Calculated Yield Strength</b>       |  |   |                    |  |   |
| Yield Strength                         | 380  | MPa   | S <sub>ys</sub>    |  | Taken to be same as "Rated Allowed Tensile Stress".   |
| Shear Yield Strength                   | 219  | MPa   | S <sub>sys</sub>   |  |   |
| <b>Actual Stresses</b>                 |  |   |                    |  |   |
| Actual shear stress                    | 121  | MPa   | wiresigmashear     | wiresigmashear=F <sub>shear</sub> /(n*A <sub>w</sub> ) |   |
| Factor of Safety against Shear of Wire | 1.8  | * NOTE: The cable's "capacity" has an inherent factor of safety of 5. |                    |  |   |

#### 2. FAILURE CHECK: EXCESSIVE TENSION OF WIRE

|  | Amount   | Unit           | Symbol             | Formula    | Source/Notes   |
|--|----------|----------------|--------------------|------------|--|
| <b>Forces</b>  |          |                |                    |            |  |
| Shear Force  | 1128.15  | N              | F <sub>shear</sub> | 115kg*9.81 |  |
| Tension Force  | 2350     | N              | T                  |            | This is the tension of the wire rope when it is tightened completely. It is calculated from section 0. |
| <b>Wire Parameters</b>                                   |          |                |                    |            |  |
| Description  |          |                |                    |            |  |
| Diameter   | 0.00318  | m              | D <sub>w</sub>     |            |  |
| Area   | 4.68E-06 | m <sup>2</sup> | A <sub>w</sub>     |            |  |
| Rated Allowed Tensile Stress                             | 380      | Mpa            | S <sub>c</sub>     |            |  |
| Number of Wires  | 2        |                | n                  |            |  |
| <b>Calculated Yield Strength</b>                         |          |                |                    |            |  |
| Yield Strength   | 380      | Mpa            | S <sub>ys</sub>    |            | Taken to be same as "Rated Allowed Tensile Stress".  |
| <b>Actual Stresses</b>                                   |          |                |                    |            |  |
| Actual tensile stress                                    | 502      | Mpa            | wiresigmatensile   |            |  |
| <b>Factor of Safety against Tensile Fracture of Wire</b> | 0.8      |                |                    |            | * NOTE: The cable's "capacity" has an inherent factor of safety of 5.                                  |



### 3. FAILURE CHECK: COMPRESSION OF RATCHET TOOTH

|               | Amount  | Unit | Symbol | Formula    | Source |
|---------------|---------|------|--------|------------|--------|
| <b>Forces</b> |         |      |        |            |        |
| Shear Force   | 1128.15 | N    | Fshear | 115kg*9.81 |        |
| Tension Force | 2350    | N    | T      |            |        |

#### Ratchet Parameters

|                                       |          |                |      |  |                      |
|---------------------------------------|----------|----------------|------|--|----------------------|
| Number of Pawls/Ratchet Teeth Engaged | 2        | n              |      |  |                      |
| Area of Compression per Ratchet Tooth | 8.06E-05 | m <sup>2</sup> | Ar_c |  | (using 1/4" by 1/2") |

#### 3. a) Material of Ratchet: PLA

|                                    |      |     |      |           |  |
|------------------------------------|------|-----|------|-----------|--|
| Yield Strength of Ratchet and Pawl | 60   | MPa | Sys  |           | Using 3D print material, PLA, properties.<br><a href="https://promolt3d.com/blogs/filament-info/82919619-pla-vs-abs-3d-printer-filament">https://promolt3d.com/blogs/filament-info/82919619-pla-vs-abs-3d-printer-filament</a> |
| Shear Yield Strength               | 34.6 | Mpa | Ssys | 0.577*Sys |  |

#### Actual Stresses

|                           |      |     |                    |                               |  |
|---------------------------|------|-----|--------------------|-------------------------------|--|
| Actual Compressive Stress | 14.6 | Mpa | ratchsigmacompress | ratchsigmacompress=T/(n*Ar_c) |  |
|---------------------------|------|-----|--------------------|-------------------------------|--|

|  |      |
|--|------|
| Factor of Safety against Buckling of Ratchet Tooth | 4.12 |
|--|------|

#### 3. b) Material of Ratchet: Stainless Steel

|                                    |       |     |      |           |  |
|------------------------------------|-------|-----|------|-----------|--|
| Yield Strength of Ratchet and Pawl | 215   | MPa | Sys  |           | Uses Ratchet from McMaster-Carr #6283K22, \$55.88/unit, Ratcheting Gear, 48 Teeth, 3" OD.<br><a href="https://www.mcmaster.com/#6283k22/=1bpqmyg">https://www.mcmaster.com/#6283k22/=1bpqmyg</a> |
| Shear Yield Strength               | 124.1 | Mpa | Ssys | 0.577*Sys | Using 304 Stainless steel, properties.<br><a href="http://asm.matweb.com/search/SpecificMaterial.asp?bassnm=mq304a">http://asm.matweb.com/search/SpecificMaterial.asp?bassnm=mq304a</a>          |

#### Actual Stresses

|                           |      |     |                    |                               |  |
|---------------------------|------|-----|--------------------|-------------------------------|--|
| Actual Compressive Stress | 14.6 | Mpa | ratchsigmacompress | ratchsigmacompress=T/(n*Ar_c) |  |
|---------------------------|------|-----|--------------------|-------------------------------|--|

|  |       |
|--|-------|
| Factor of Safety against Buckling of Ratchet Tooth | 14.75 |
|--|-------|

#### 4. FAILURE CHECK: SHEAR OF RATCHET TOOTH

|               | Amount    | Unit | Symbol             | Formula    | Source |
|---------------|-----------|------|--------------------|------------|--------|
| <b>Forces</b> |           |      |                    |            |        |
| Shear Force   | 1128.15   | N    | F <sub>shear</sub> | 115kg*9.81 |        |
| Tension Force | 2350.3125 | N    | T                  |            |        |

##### Ratchet Parameters

|                                       |          |                |                 |  |  |
|---------------------------------------|----------|----------------|-----------------|--|--|
| Number of Pawls/Ratchet Teeth Engaged | 2        |                | n               |  |  |
| Total Number of Ratchet Teeth         | 48       |                |                 |  |  |
| Degree per Ratchet Tooth              | 0.1309   | radians        |                 |  |  |
| Minor Diam of Ratchet                 | 2        | in             |                 |  |  |
|                                       | 0.0508   | m              |                 |  |  |
| Thickness of Ratchet Face             | 0.25     | in             |                 |  |  |
|                                       | 0.00635  | m              |                 |  |  |
| Area of Shear per Ratchet Face        | 2.11E-05 | m <sup>2</sup> | Ar <sub>s</sub> |  |  |

##### 3. a) Material of Ratchet: PLA

|                                    |      |     |      |           |  |
|------------------------------------|------|-----|------|-----------|--|
| Yield Strength of Ratchet and Pawl | 60   | MPa | Sys  |           |  |
| Shear Yield Strength               | 34.6 | MPa | Ssys | 0.577*Sys |  |

Using 3D print material, PLA, properties.  
<https://promolt3d.com/blogs/filament-info/82919619-pla-vs-abs-3d-printer-filament>

##### Actual Stresses

|              |      |     |                 |                                    |  |
|--------------|------|-----|-----------------|------------------------------------|--|
| Shear Stress | 55.7 | Mpa | ratchsigmashear | $ratchsigmashear = T / (n * Ar_s)$ |  |
|--------------|------|-----|-----------------|------------------------------------|--|

|   |      |
|---|------|
| <b>Factor of Safety against Shearing of Ratchet Tooth</b> | 0.62 |
|---|------|

##### 3. b) Material of Ratchet: Stainless Steel

|                                    |       |     |      |           |  |
|------------------------------------|-------|-----|------|-----------|--|
| Yield Strength of Ratchet and Pawl | 215   | MPa | Sys  |           |  |
| Shear Yield Strength               | 124.1 | MPa | Ssys | 0.577*Sys |  |

Using 304 Stainless steel, properties.  
<http://asm.matweb.com/search/SpecificMaterial.asp?bassnum=mq304a>

##### Actual Stresses

|                           |      |     |                 |                                    |  |
|---------------------------|------|-----|-----------------|------------------------------------|--|
| Actual Compressive Stress | 55.7 | Mpa | ratchsigmashear | $ratchsigmashear = T / (n * Ar_s)$ |  |
|---------------------------|------|-----|-----------------|------------------------------------|--|

|   |      |
|---|------|
| <b>Factor of Safety against Shearing of Ratchet Tooth</b> | 3.86 |
|---|------|

#### 5. FAILURE CHECK: FATIGUE

| Properties of 18-8 Stainless steel | Amount | Unit | Symbol | Formula | Source |
|------------------------------------|--------|------|--------|---------|--------|
| Ultimate Tensile Strength          | 505    | Mpa  | Sut    |         |        |
|                                    | 73.2   | ksi  |        |         |        |
| Yield Strength                     | 215    | Mpa  | Sy     |         |        |
| Elongation at break                | 70%    |      |        |         |        |
| Elastic Modulus                    | 193    | Mpa  | E      |         |        |
|                                    | to 200 |      |        |         |        |
| Poisson Ratio                      | 0.29   |      | v      |         |        |
| Shear Modulus                      | 86     | Gpa  | G      |         |        |

##### Calculating Endurance Strength

|                    |       |            |             |  |  |
|--------------------|-------|------------|-------------|--|--|
| Se'                | 252.5 | Mpa        | Se'=0.5*Sut |  | Eq 6-8 of Shigley's (2015).  |
| ka                 | 0.867 | 0.55564061 | ka=a*Sut^b  |  | Eq 6-19 and Table 6-2 of Shigley's (2015),<br>Take "as forged" condition, a= 272, b=-0.995 |
| kb                 | 1     |            |             |  | Eq 6-21 of Shigley's (2015), because axial.  |
| kc                 | 0.85  |            |             |  | Eq 6-26 of Shigley's (2015), because axial.  |
| kd                 | 1     |            |             |  | Temperature modifier considered negligible.  |
| ke                 | 1     |            |             |  | Reliability modifier considered negligible.  |
| kf                 | 1     |            |             |  | Stress concentration factor modifier considered negligible.                                |
| Endurance Strength | 186   | Mpa        | Se          | $Se = Se' * ka * kb * kc * kd * ke * kf$ |  |

##### Calculating Fatigue FS

|                        |          |                |    |  |  |
|------------------------|----------|----------------|----|--|--|
| Tensile area           | 4.68E-06 | m <sup>2</sup> | At |  |  |
| External Tensile Force | 2350     | N              | P  |  |  |

|                                 |       |     |  |  |  |
|---------------------------------|-------|-----|--|--|--|
| <b>Fatigue Factor of Safety</b> | 0.541 | nf0 |  |  | Eq 8-49 of Shigley's (2015), assumes no preload so F <sub>i</sub> =0, C=1. |
|---------------------------------|-------|-----|--|--|--|

## 6. FAILURE CHECK: SHEAR OF PIN

Description: The bolt pinning the ends of the cable down (i.e. on the other side of the longboard than the ratchet) must be able to withstand the tensile force of the cable that could shear the bolt/pin.

Key Formulas:  $\text{Shearstress} = F_{\text{shear}} / (\pi \cdot d^2 / 4)$ ,  
 where  $d$  is the nominal diameter of the bolt.  
 $\text{Shearstress} < \text{Shearyieldstrength} / \text{designfactor}$   
 To find diameter,  $d > \sqrt{4 \cdot \pi \cdot F_{\text{shear}} / (S_{\text{sys}} / n_d)}$

|                                   | <u>Amount</u>                 | <u>Unit</u> | <u>Symbol</u> | <u>Formula</u>   | <u>Source/Notes</u>   |
|-----------------------------------|-------------------------------|-------------|---------------|--|---|
| <b>Forces</b>                     |                               |             |               |  |   |
| Shear Force (tensile)             | 2350.3125                     | N           | Fshear        |  |   |
| <b>Bolt Parameters</b>            |                               |             |               |  |   |
| Yield Strength                    | 350                           | MPa         | Sys           |  | <a href="http://www.matweb.com/search/datasheet.aspx?bassnum=MS0001&amp;ckck=1">http://www.matweb.com/search/datasheet.aspx?bassnum=MS0001&amp;ckck=1</a> |
| Shear Yield Strength              | 202                           | MPa         | Ssys          |  |   |
| <b>Other Parameters</b>           |                               |             |               |  |   |
| Design factor                     | 4                             |             | nd            |  |   |
| <b>Required Diameter</b>          |                               |             |               |  |   |
| Min Bolt Diameter                 | 0.00769885 m<br>0.30310455 in |             | mind          | $d>\sqrt{4/\pi * F_{\text{shear}}/(S_{\text{sys}}/n_d)}$ |   |
| <b>Closest Standard Bolt Size</b> | 5/16"                         | in          | d             |  |   |

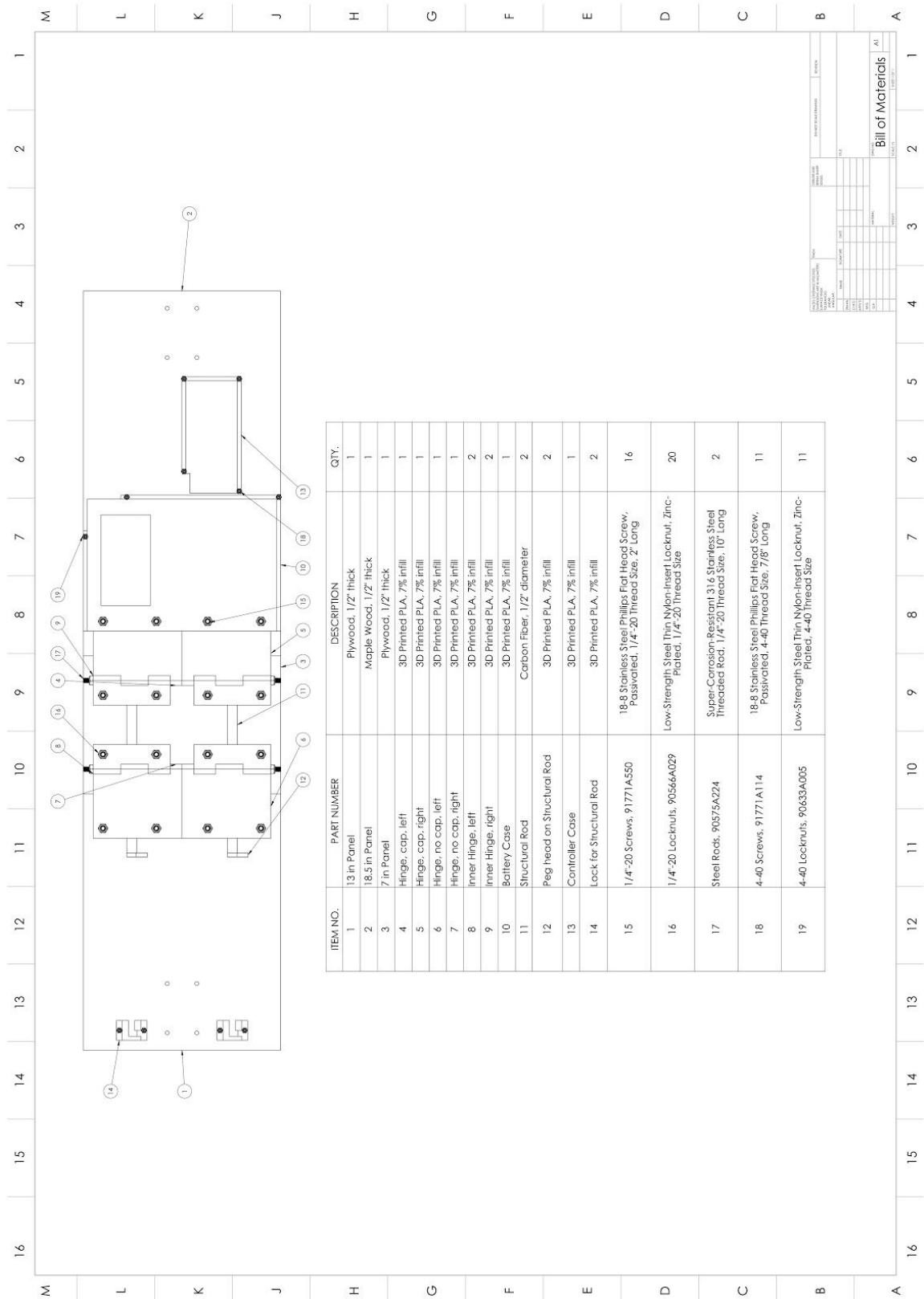
\*Note: the 1/4" bolts that will be used for the ratchet will not suffice.

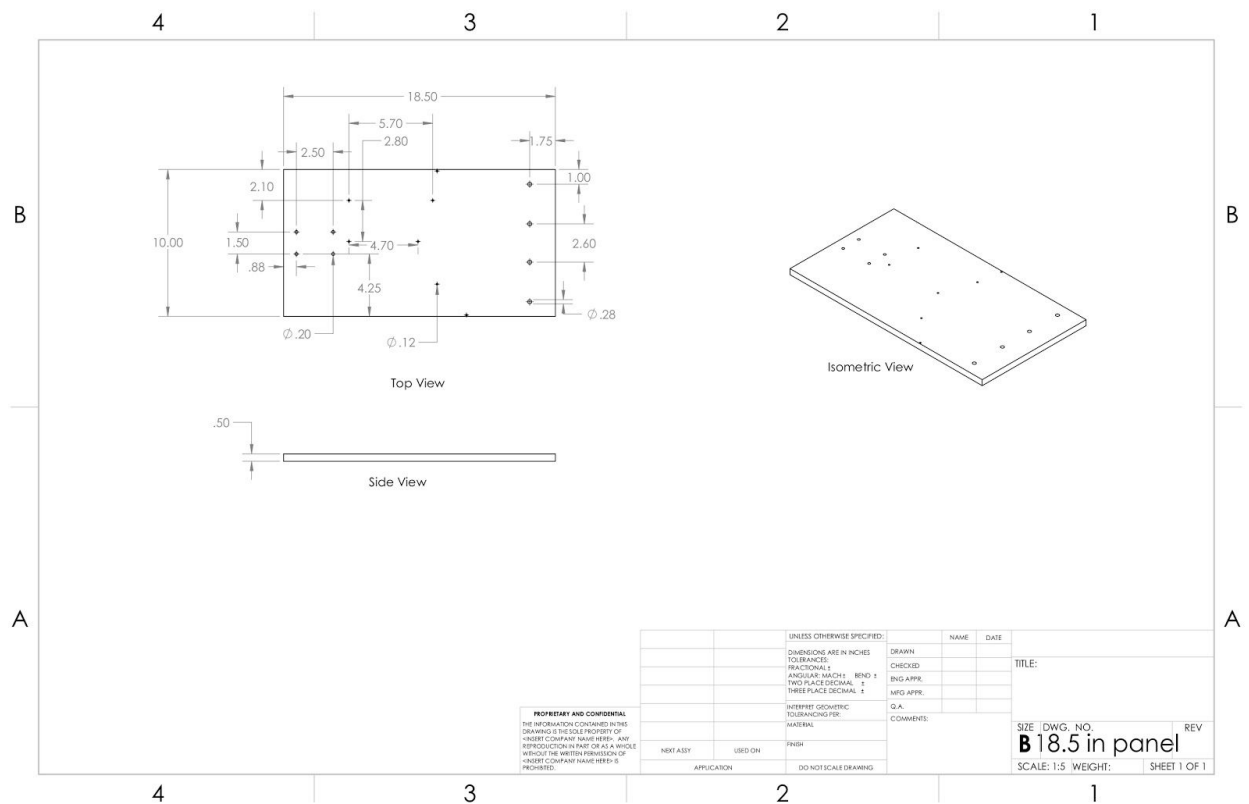
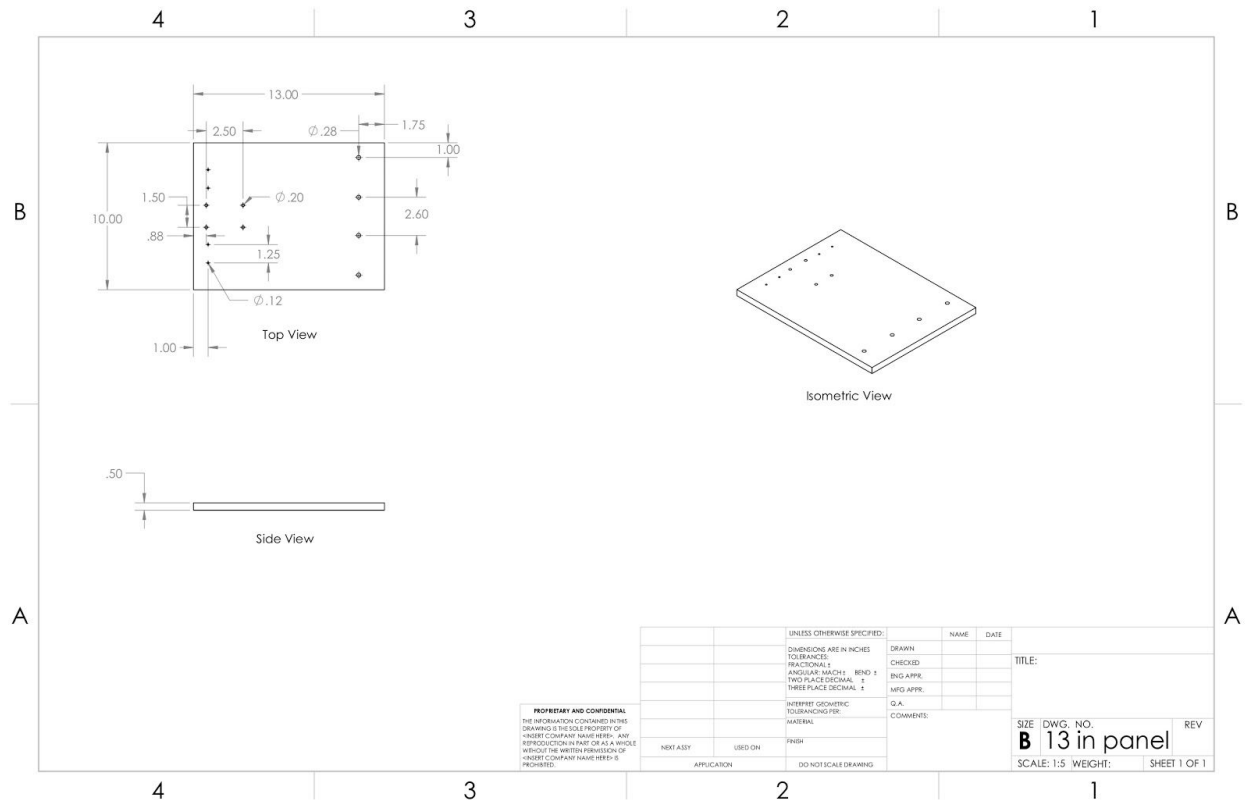
## EXTRA CHECKS: 1. COMPRESSIVE/TENSILE FORCE FROM BENDING FOUND TO BE NEGLIGIBLE

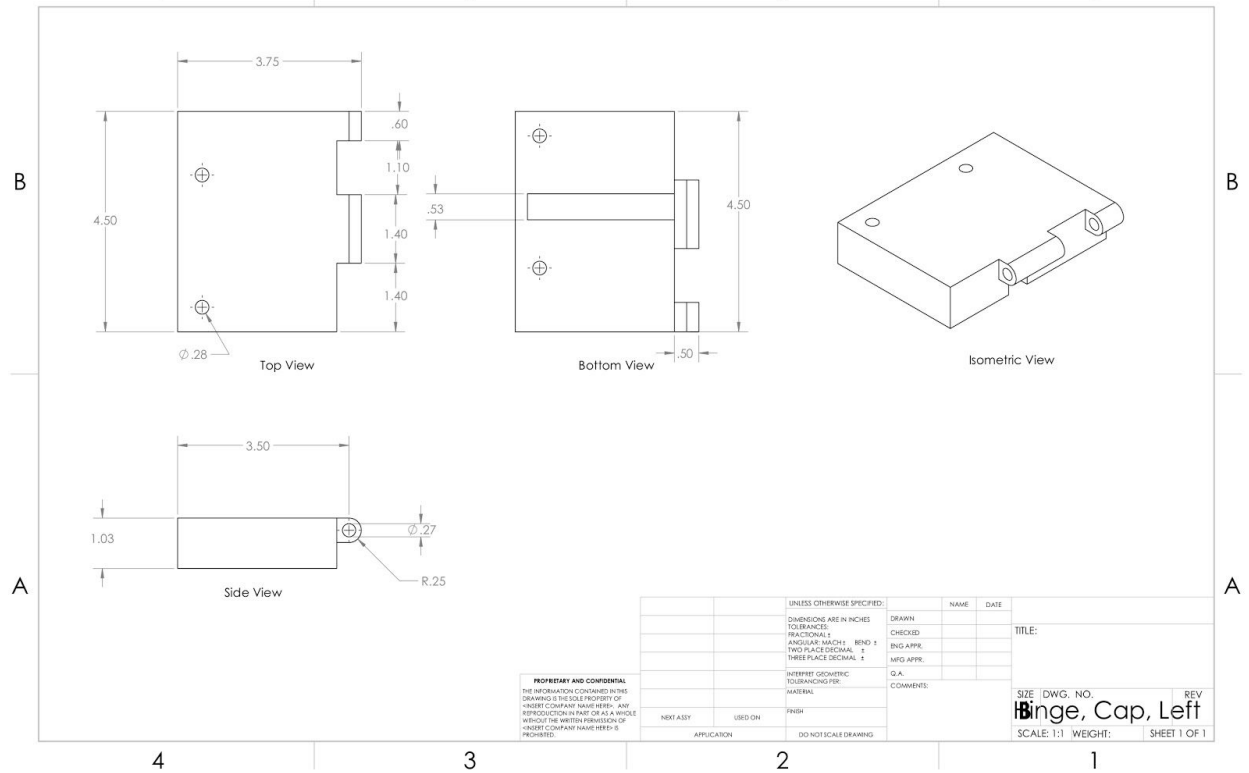
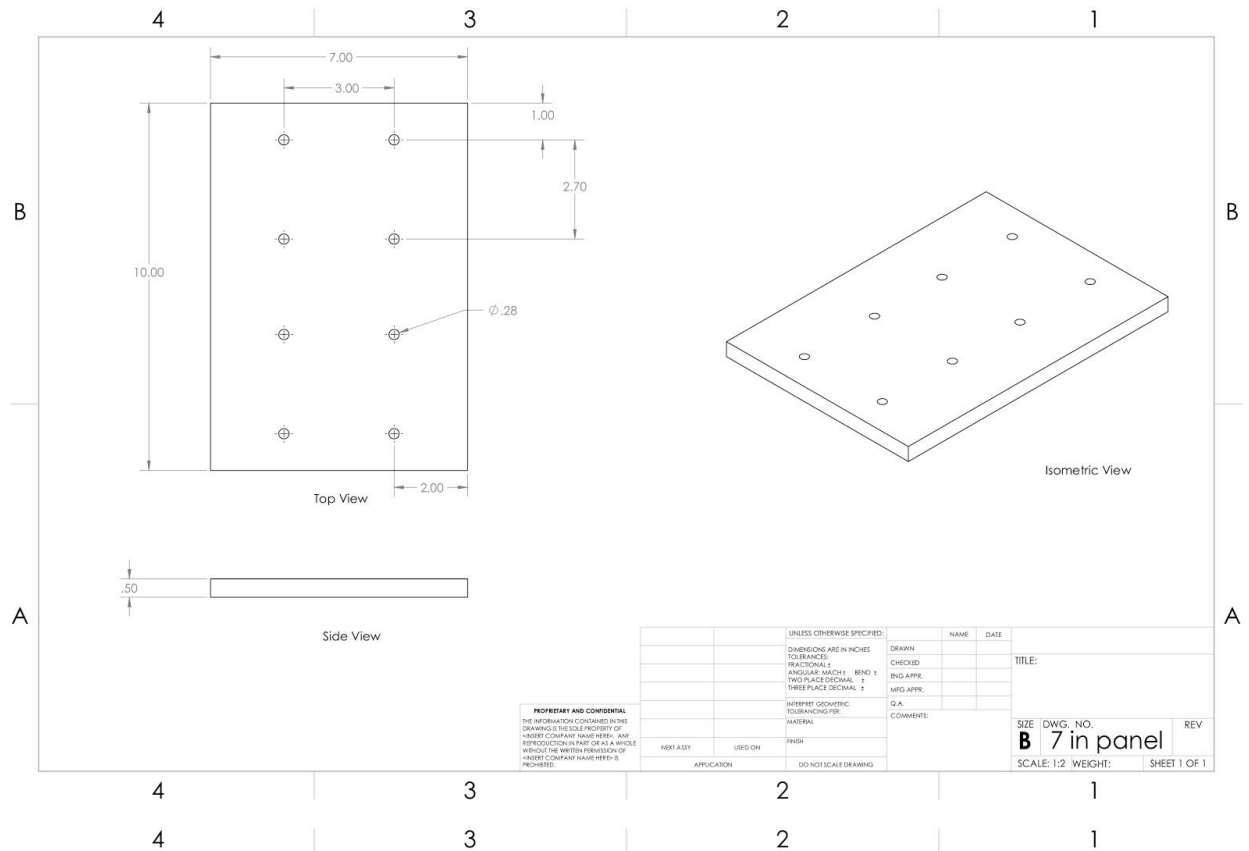
Description: A check to see if the the compression within the wire from it bending as a result of someone standing on it will overcome the tension the wire is in, which would not be desired. Therefore, this bending stress was checked but was found to be negligible.

|                                     | Amount          | Unit              | Symbol                | Formula                                       | Source/Notes  |
|-------------------------------------|-----------------|-------------------|-----------------------|---|---|
| <b>Finding Tensile from Bending</b> |                 |                   |                       |   |   |
| Length of Board                     | 36 in<br>0.86 m |                   | $L$                   |   |   |
| Moment Arm                          | 0.43 m          |                   | $R$                   |   |   |
| Force Exerted                       | 1128.15         | N                 | $F$                   |   |   |
| Moment                              | 487             | Nm                | $M$                   |   |   |
| Thickness of wire                   | 0.00318         | m                 | $D_w$                 |   |   |
| Max Distance from Neutral Axis      | 0.00159         | m                 | $c$                   |   |   |
| Volume                              | 4.04E-06        | m <sup>3</sup>    | $V$                   | $V = A_w \cdot L$                             |   |
| Density of stainless steel          | 7700            | kg/m <sup>3</sup> | $\rho$                |   | <a href="https://www.engineeringtoolbox.com/metal-alloys-densities-d_50.html">https://www.engineeringtoolbox.com/metal-alloys-densities-d_50.html</a> |
| Mass                                | 0.0311          | kg                | $M_a$                 |   |   |
| Second-Area Moment of Inertia       | 0.00194         | m <sup>4</sup>    | $I$                   | $I_{\text{rod}} = 1/12 \cdot (M_a \cdot L^2)$ |   |
| Max Compressive Stress from Bending | 0.0255          | N/m <sup>2</sup>  | $\text{bendingsigma}$ | $\text{bendingsigma} = M_c / I$               | Eq 3-26a of Shigley's (2015).   |

Appendix 2. Final Design Drawings



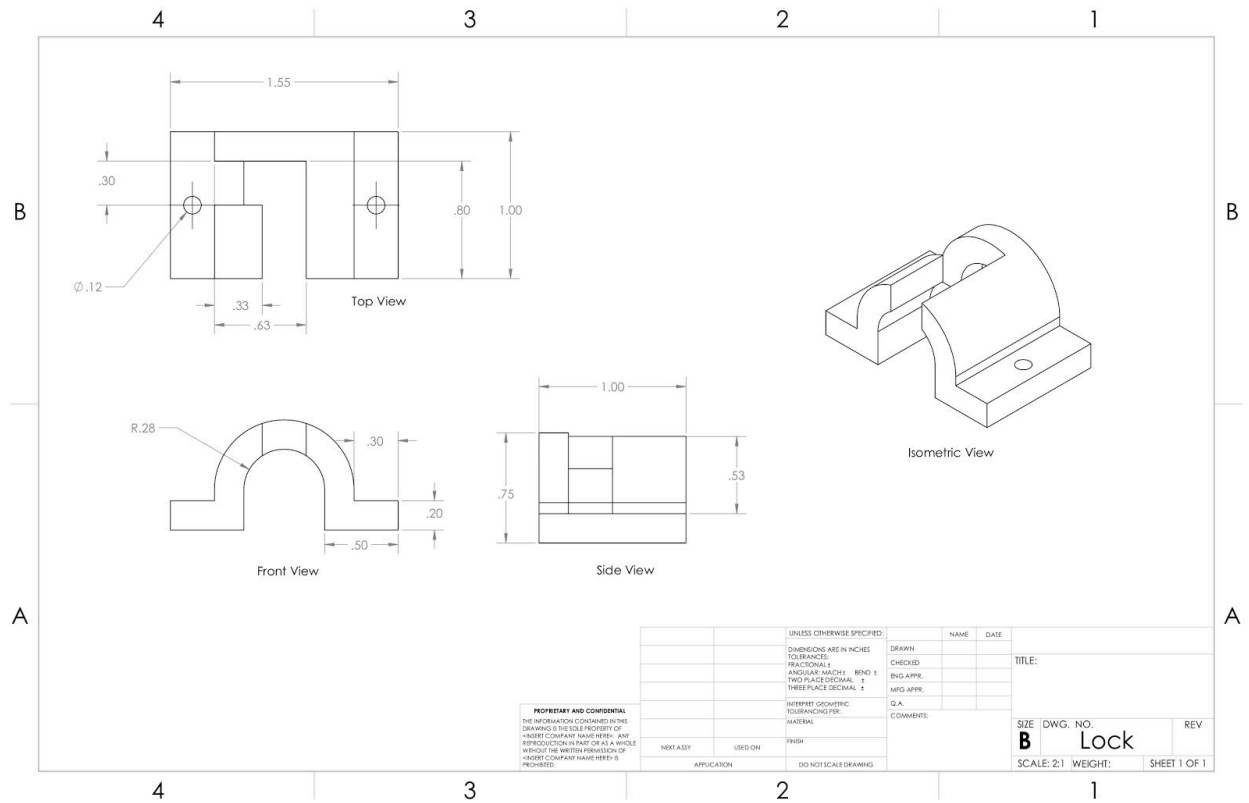










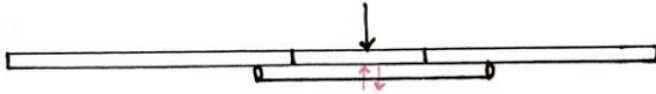


## Appendix 3. Final Design Stress Analysis

### Appendix 3.1. Stress Analysis Excel Calculations

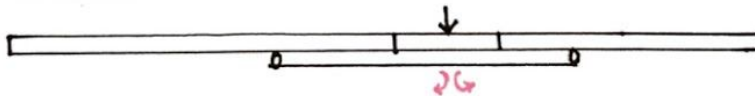
#### 1. FAILURE CHECK: Structural Rods

Figure 1: Shear of structural rod/beam diagram



|   |                     |             |               |                                   |   |  |
|---|---------------------|-------------|---------------|-----------------------------------|---|--|
| <b>1.A. Shear of Steel Rods</b>   |                     |             | Part Link:    |                                   | <a href="https://www.mcmaster.com/#90575a224/=1cca0x5">https://www.mcmaster.com/#90575a224/=1cca0x5</a>   |  |
| <b>Description:</b> A check of whether the steel rods used in the hinges would shear from the weight of a person. |                     |             |               |                                   |   |  |
| <b>Rod Parameters</b>   | <u>Amount</u>       | <u>Unit</u> | <u>Symbol</u> | <u>Formula</u>                    | <u>Source/Notes</u>   |  |
| Number of Rods  | 2                   |             | nRod          |                                   |   |  |
| Diameter of Rod   | 0.25 in             |             | dRod          |                                   | Given by McMaster-Carr  |  |
|   | 0.00635 m           |             |               |                                   |   |  |
| Cross-sectional area of Rod   | 0.0491 in^2         |             | ARod          | pi*dRod^2/4                       |   |  |
|   | 3.17E-05 m^2        |             |               |                                   |   |  |
| Material  | 316 Stainless Steel |             |               |                                   | Given by McMaster-Carr  |  |
| Rated Ultimate Tensile Strength   | 70,000 psi          |             | Sut           |                                   | Given by McMaster-Carr  |  |
|   | 4.83E+08 Pa         |             |               |                                   |   |  |
| Tensile Yield Strength  | 42,100 psi          |             | Sy            |                                   | <a href="http://asm.matweb.com/search/SpecificMaterial.asp?bassnum=mq316a">http://asm.matweb.com/search/SpecificMaterial.asp?bassnum=mq316a</a> |  |
|   | 2.90E+08 Pa         |             |               |                                   |   |  |
| Shear Yield Strength  | 24,292 psi          |             | Sys           | 0.577*Sy                          |   |  |
|   | 1.67E+08 Pa         |             |               |                                   |   |  |
| <b>Forces and Stresses</b>  | <u>Amount</u>       | <u>Unit</u> | <u>Symbol</u> | <u>Formula</u>                    | <u>Source/Notes</u>   |  |
| Shear Force   | 253.618 lbf         |             | Weight        | 115kg*9.81 m/s^2 converted to lbf | All analyses use this force.  |  |
|   | 1128.15 N           |             |               |                                   |   |  |
| Shear Stress  | 2,583 psi           |             |               |                                   |   |  |
|   | 1.8E+07 Pa          |             |               |                                   |   |  |
| <b>Factor of Safety</b>   | <b>9.40</b>         |             |               | Sys/Shear Stress                  |   |  |

Figure 2: Bending of structural rod/beam diagram



|   |                |              |            |  |                               |
|---|----------------|--------------|------------|--|-------------------------------|
| 1.B. Bending of Steel Rods  |                |              | Part Link: | <a href="https://www.mcmaster.com/#90575a224/=1cca05">https://www.mcmaster.com/#90575a224/=1cca05</a>                    |                               |
| Description: A check of whether the steel rods used in the hinges would bend plastically from the weight of a person.           |                |              |            |  |                               |
| Finding Tensile from Bending  | Amount         | Unit         | Symbol     | Formula  | Source/Notes                  |
|   |                |              |            | Distance from the edge of the hinge to the center of the middle panel. This is the portion where the rod is not secured. |                               |
| Moment Arm  | 1.00 in        |              |            |  |                               |
|   | 0.0254 m       | R            |            |  |                               |
| Force Exerted   | 564.075 N      | F            |            | Weight/nRod  |                               |
| Moment  | 14.3 Nm        | M            |            | F*R  |                               |
| Max Distance from Neutral Axis  | 0.00318 m      | c            |            | dRod/2   |                               |
| Centroidal Moment of Inertia  | 7.98E-11 m^4   | Ic           |            | Ic=pi*d^4/64   | For a circular cross-section  |
| Max Tensile Stress from Bending   | 5.70E+08 N/m^2 | bendingsigma |            | bendingsigma=Mc/I  | Eq 3-26a of Shigley's (2015). |
| Factor of Safety  | 0.51           |              |            | Sy/bendingsigma  |                               |
| Conclusion: Since the rods will plastically bend, we will look into the alternatives, a Carbon Fiber Rod or a Carbon Fiber Bar. |                |              |            |  |                               |

|  |                           |             |               |  |                               |
|--|---------------------------|-------------|---------------|--|-------------------------------|
| 1.C. Bending of Carbon Fiber Rods  |                           |             | Part Link:    | <a href="https://www.mcmaster.com/#2153t58/=1ccbfit">https://www.mcmaster.com/#2153t58/=1ccbfit</a>                      |                               |
| <b>Beam Parameters</b>   | <u>Amount</u>             | <u>Unit</u> | <u>Symbol</u> | <u>Formula</u>   | <u>Source/Notes</u>           |
| Number of Rods   | 2                         |             | nRod          |  |                               |
| Diameter of Rod  | 0.5 in                    |             | dRod          |  |                               |
|  | 0.0127 m                  |             |               |  |                               |
| Cross-sectional area of Rod  | 0.196 in <sup>2</sup>     |             | ARod          | $\pi \cdot d_{Rod}^2/4$  |                               |
|  | 0.000127 m <sup>2</sup>   |             |               |  |                               |
| Length of rod  | 12 in                     |             | IRod          |  |                               |
|  | 0.305 m                   |             |               |  |                               |
| Material   | Carbon Fiber              |             |               |  |                               |
| Rated Flexural Strength  | 89,000 psi                |             | FlexuralSy    |  |                               |
|  | 6.14E+08 Pa               |             |               |  |                               |
| <b>Finding Tensile from Bending</b>  | <u>Amount</u>             | <u>Unit</u> | <u>Symbol</u> | <u>Formula</u>   |                               |
|  |                           |             |               | Distance from the edge of the hinge to the center of the middle panel. This is the portion where the rod is not secured. |                               |
| Moment Arm   | 1.00 in                   |             |               |  |                               |
|  | 0.0254 m                  |             | R             |  |                               |
| Force Exerted  | 564.075 N                 |             | F             | Weight/nRod  |                               |
| Moment   | 14.3 Nm                   |             | M             | F*R  |                               |
| Max Distance from Neutral Axis   | 0.00635 m                 |             | c             | dRod/2   |                               |
| Centroidal Moment of Inertia   | 1.28E-09 m <sup>4</sup>   |             | Ic            | $Ic = \pi \cdot d^4/64$  | For a circular cross-section  |
| Max Tensile Stress from Bending  | 7.12E+07 N/m <sup>2</sup> |             | Bendingsigma  | $M \cdot c/Ic$   | Eq 3-26a of Shigley's (2015). |
| <b>Factor of Safety</b>  | <b>8.61</b>               |             |               | FlexuralSy/Bendingsigma  |                               |
| <b>Conclusion:</b> This is a sufficient factor of safety. We will still look into using a carbon fiber bar to see if it is better. |                           |             |               |  |                               |

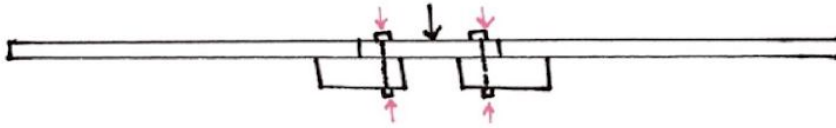
|  |                           |             |               |  |                                 |
|--|---------------------------|-------------|---------------|--|---------------------------------|
| 1.D. Bending of Carbon Fiber Bars  |                           |             | Part Link:    | <a href="https://www.mcmaster.com/#2153t28/=1ccb9xu">https://www.mcmaster.com/#2153t28/=1ccb9xu</a>                      |                                 |
| <b>Beam Parameters</b>   | <u>Amount</u>             | <u>Unit</u> | <u>Symbol</u> | <u>Formula</u>   |                                 |
| Number of Rods   | 2                         |             | nBar          |  |                                 |
| Thickness of beam  | 0.125 in                  |             | hBar          |  |                                 |
|  | 0.00318 m                 |             |               |  |                                 |
| Width of beam  | 0.5 in                    |             | wBar          |  |                                 |
|  | 0.0127 m                  |             |               |  |                                 |
| Length of beam   | 12 in                     |             | lBar          |  |                                 |
|  | 0.305 m                   |             |               |  |                                 |
| Cross-sectional area of Rod  | 0.0625 in <sup>2</sup>    |             | ARod          |  |                                 |
|  | 4.03E-05 m <sup>2</sup>   |             |               |  |                                 |
| Material   | Carbon Fiber              |             |               |  |                                 |
| Rated Flexural Strength  | 89,000 psi                |             |               |  |                                 |
|  | 6.14E+08 Pa               |             |               |  |                                 |
| <b>Finding Tensile from Bending</b>  | <u>Amount</u>             | <u>Unit</u> | <u>Symbol</u> | <u>Formula</u>   |                                 |
|  |                           |             |               | Distance from the edge of the hinge to the center of the middle panel. This is the portion where the rod is not secured. |                                 |
| Moment Arm   | 1.00 in                   |             |               |  |                                 |
|  | 0.0254 m                  |             | R             |  |                                 |
| Force Exerted  | 564.075 N                 |             | F             | Weight/nBar  |                                 |
| Moment   | 14.3 Nm                   |             | M             | F*R  |                                 |
| Max Distance from Neutral Axis   | 0.00159 m                 |             | c             | hBar/2   |                                 |
| Centroidal Moment of Inertia   | 3.39E-11 m <sup>4</sup>   |             | Ic            | $Ic_x = wBar \cdot hBar^3/12$  | For a rectangular cross-section |
| Max Tensile Stress from Bending  | 6.71E+08 N/m <sup>2</sup> |             | Bendingsigma  | $M \cdot c/Ic_x$   | Eq 3-26a of Shigley's (2015).   |
| <b>Factor of Safety</b>  | <b>0.91</b>               |             |               | FlexuralSy/Bendingsigma  |                                 |
| <b>Conclusion:</b> This would fail. The carbon fiber rod is the best solution to deal with bending stress. We will now go back and see if it will survive the shear force. |                           |             |               |  |                                 |

|   |               |             |               |   |   |
|---|---------------|-------------|---------------|---|---|
| <u>1.E. Shear of Carbon fiber Rods</u>  |               |             | Part Link:    | <a href="https://www.mcmaster.com/#2153t58/=1ccbfit">https://www.mcmaster.com/#2153t58/=1ccbfit</a> |   |
| <b>Description:</b> A check of whether the carbon fiber rods would shear from the weight of a person. |               |             |               |   |   |
| <b>Rod Parameters</b>   | <u>Amount</u> | <u>Unit</u> | <u>Symbol</u> | <u>Formula</u>  | <u>Source/Notes</u>   |
| Number of Rods  | 2             |             | nRod          |   |   |
| Diameter of Rod   | 0.5 in        |             | dRod          |   |   |
|   | 0.0127 m      |             |               |   |   |
| Cross-sectional area of Rod   | 0.196 in^2    |             | ARod          | pi*dRod^2/4   |   |
|   | 0.000127 m^2  |             |               |   |   |
| Material  | Carbon Fiber  |             |               |   |   |
| Rated Ultimate Tensile Strength   | 120,000 psi   |             | Sut           |   | McMaster-Carr advises to use the strength properties of Aluminum 6061,  |
|   | 8.27E+08 Pa   |             |               |   | <a href="http://asm.matweb.com/search/SpecificMaterial.asp?bassnum=ma6061t6">http://asm.matweb.com/search/SpecificMaterial.asp?bassnum=ma6061t6</a> |
| Tensile Yield Strength  | 40,000 psi    |             | Sy            |   |   |
|   | 2.76E+08 Pa   |             |               |   |   |
| Shear Yield Strength  | 30,000 psi    |             | Sys           | 0.577*Sy  |   |
|   | 2.07E+08 Pa   |             |               |   |   |
| <b>Forces and Stresses</b>  | <u>Amount</u> | <u>Unit</u> | <u>Symbol</u> | <u>Formula</u>  | <u>Source/Notes</u>   |
| Shear Force   | 253.618 lbf   |             | Weight        | 115kg*9.81 m/s^2 converted to lbf   |   |
|   | 1128.15 N     |             |               |   |   |
| Shear Stress  | 646 psi       |             |               |   |   |
|   | 4.45E+06 Pa   |             |               |   |   |
| <b>Factor of Safety</b>   | <b>46.5</b>   |             |               | Sys/Shear Stress  |   |
| <b>Conclusion:</b> The carbon fiber rods will not shear from the weight of a person.                  |               |             |               |   |   |

## 2. FAILURE CHECK: PLA under Bolt Pretension

**Description:** We have to find the amount of pretension needed in the bolt to keep the PLA clamped to the wood when someone stands on it. The worst case scenario is that the 8 bolts on the center panel take all of the weight of the person. We will make calculations based on this worst case scenario.

Figure 3: Free-Body diagram with bolt reactions



### 2.A Finding Pretension through Proof Strength

| Parameters          | Amount   | Unit            | Symbol | Formula               | Source/Notes  |
|---------------------|----------|-----------------|--------|-----------------------|---|
| Major Diameter      | 0.25     | in              |        |                       |   |
|                     | 0.00635  | m               |        |                       |   |
| Threads per inch    | 20       |                 |        |                       |   |
| Thread Type         | UNC      |                 |        |                       |   |
| Tensile Stress Area | 0.0318   | in <sup>2</sup> |        |                       | Table 8-2 of Shigley's (2015), p.405  |
|                     | 2.05E-05 | m <sup>2</sup>  |        |                       |   |
| Proof Strength      | 135,000  | psi             |        |                       | McMaster-Carr notes the bolts meet ASTM A574 specifications. Referring to p.9 of the Technical Reference Guide (2005) by Fastenal Industrial & Construction Supplies, <a href="https://www.fastenal.com/content/documents/FastenalTechnicalReferenceGuide.pdf">https://www.fastenal.com/content/documents/FastenalTechnicalReferenceGuide.pdf</a> , since it is above 1/2" in length, its proof-strength is 135ksi. |
|                     | 9.31E+08 | Pa              | Sp     |                       |   |
| Proof Load          | 1.91E+04 | N               | Fp     | $F_p = A_t \cdot S_p$ | Eq 8-32 of Shigley's (2015), p.434  |
| Pretension Force    | 1.72E+04 | N               | Fi     | $F_i = 0.9 \cdot F_p$ | Eq 8-31 of Shigley's (2015), p.434  |

**Conclusion:** This pretension load is unnecessary and will likely damage the PLA. The purpose of pretension is to concentrate the majority of the load on the bolt, but this is not needed. The structural rods should take the majority of the weight of the person. Whereas the bolts are there purely to keep the PLA and wood clamped together. Thus pretension only needs to compress the PLA and wood enough so that when the weight of a person is applied, it is still greater than the tension created between the PLA and wood.

### 2.B. Finding Pretension through Clamping Force Needed

| Parameters                                | Amount  | Unit | Symbol | Formula   | Source/Notes                        |
|---|---------|------|--------|---|-------------------------------------|
| Number of Bolts                           | 8       |      |        |   |                                     |
| Tension Force between PLA and Wood        | 253.618 | lbf  | Weight | $115\text{kg} \cdot 9.81\text{ m/s}^2$ converted to lbf |                                     |
|   | 1128.15 | N    |        |   |                                     |
| Min Pretension Force Needed per Bolt      | 141.019 | N    | minFi  |   |                                     |
| Factor of Safety Against Joint Separation | 5       |      | n0     |   | Eq 8-29e of Shigley's (2015), p.433 |
| Pretension per Bolt                       | 705.094 | N    | Fi     | $n0 \cdot \text{minFi}$                                 |                                     |

### 2.C. Failure Check of Whether PLA from Compression

**Description:** We are finding whether the PLA can withstand the compression from the pretension in the bolt.

| Parameters                        | Amount      | Unit           | Symbol | Formula | Source/Notes  |
|-----------------------------------|-------------|----------------|--------|---------|---|
| PLA Compressive Yield Strength    | 2600        | psi            |        |         | <a href="http://2015.igem.org/wiki/images/2/24/CamJIC-Specs-Strength.pdf">http://2015.igem.org/wiki/images/2/24/CamJIC-Specs-Strength.pdf</a> |
|                                   | 1.79E+07    | Pa             |        |         |   |
| Nut Width                         | 0.4375      | in             |        |         | <a href="https://www.mcmaster.com/#94895a029/=1cdtmyy">https://www.mcmaster.com/#94895a029/=1cdtmyy</a>                                       |
|                                   | 0.0111      | m              |        |         |   |
| Interface Area                    | 9.699E-05   | m <sup>2</sup> |        |         |   |
| Max Compressive Stress in Plastic | 7.27E+06    | Pa             |        |         |   |
| <b>Factor of Safety</b>           | <b>2.47</b> |                |        |         |   |

**Conclusion:** The PLA is safe against compression from the pretension in the bolt.

### 3. FAILURE CHECK: Fatigue

**Description:** The major structure taking the load is the carbon fiber rods. These carbon fiber rods must be able to withstand many load cycles where the load goes from zero to the weight of a person when someone steps on and off. Carbon Fiber is similar to Aluminium in that it does not have a fatigue limit. McMaster-Carr advises using Aluminium 6061 for the carbon fiber rod's strength properties. Using the fatigue strength and life of Aluminium 6061, the rods life is virtually infinite. The highest stress experienced by the carbon fiber rods is that from bending ( $7.12 \times 10^7$  Pa, as compared to its max shear stress of  $4.45 \times 10^6$  Pa).

|                               | Amount         | Unit             | Symbol                 | Formula           | Source/Notes   |
|-------------------------------|----------------|------------------|------------------------|-------------------|--|
| Max Bending Stress            | 71.25          | MPa              | bendingsigma           | $M \cdot c / I_c$ | From structural rod calculations.<br><br><a href="http://asm.matweb.com/search/SpecificMaterial.asp?bassnum=ma6061t6">http://asm.matweb.com/search/SpecificMaterial.asp?bassnum=ma6061t6</a> , note that the fatigue strength is higher than the max bending stress. |
| Fatigue Strength/Fatigue Life | 96.5           | MPa              | For 500 million cycles |                   | Assumptions: 2 Trips per day, 4 stops per trip, used every day of the year.  |
| Estimated Number of Cycles Pe | 2920           | Load cycles/year |                        |                   |  |
| <b>Estimated Life</b>         | <b>171,233</b> | <b>years</b>     |                        |                   |  |

### 4. FAILURE CHECK: PLA under Rods Compression + FEA

**Description:** The rods exert a force on the PLA hinge when someone stands on the board. This compressive stress in the PLA caused by the transmission of the persons weight is too complicated to do by hand because of the unique part shapes and materials. Thus, a finite element analysis (FEA) was run to estimate the stress in the PLA. Please refer to the FEA results for the simplified build out of the design, assumptions made, materials used, and any other additional information.

| Parameters  | Amount       | Unit             | Symbol | Formula | Source/Notes   |
|---|--------------|------------------|--------|---------|--|
| Max Von Mises Stress in PLA   | 3.15E+06     | N/m <sup>2</sup> |        |         | This was found through probing all faces of the PLA hinges and then finding the maximum Von Mises stress across them. The FEA assumes an infill density of 100%. Thus, the final design uses a prototype with 90% infill density. This should mimic the strength properties of a solid PLA print, without severely hindering the quality of the print. Printing at 90% infill density will only add 1.5lb to the total weight of the system. |
| PLA Strength with 90% Infill Density, 0.25 layer height                         | 4.20E+07     | Pa               |        |         | <a href="http://my3dmatter.com/influence-infill-layer-height-pattern/">http://my3dmatter.com/influence-infill-layer-height-pattern/</a>  |
| <b>Factor of Safety, 90% Infill</b>   | <b>13.33</b> |                  |        |         |  |
| PLA Strength with 100% Infill Density, 0.2 layer height                         | 4.60E+07     | Pa               |        |         | <a href="http://my3dmatter.com/influence-infill-layer-height-pattern/">http://my3dmatter.com/influence-infill-layer-height-pattern/</a>  |
| <b>Factor of Safety, 100% Infill</b>  | <b>14.59</b> |                  |        |         |  |
| <b>Conclusion:</b> The 90% Infill suffices. 100% infill density is unnecessary. |              |                  |        |         |  |

## Appendix 3.2. Finite Element Analysis

### FEA Setup

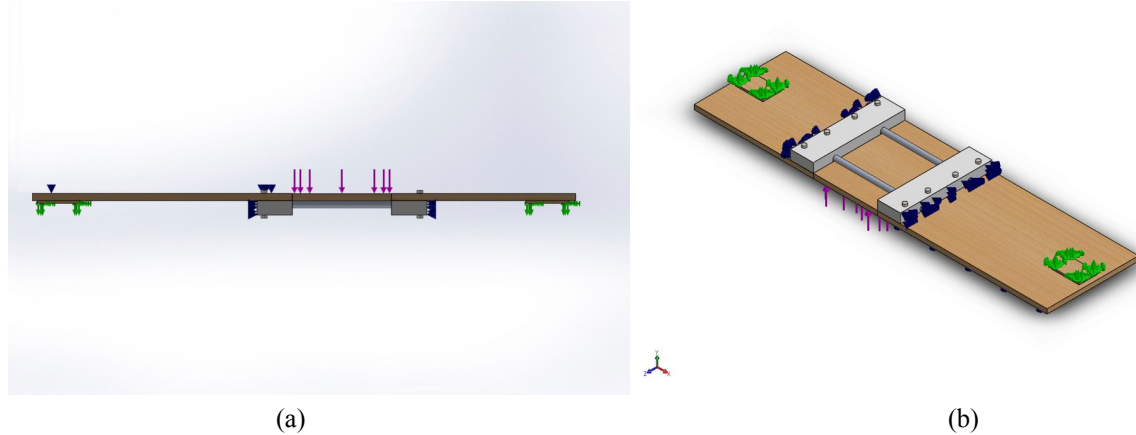


Figure 1: (a) Side view of simulation setup. (b) Perspective view of simulation setup.

**Simplification of Model:** We initially tried running the simulation on the final design but the complex design created numerous errors that crashed simulations. The second time running the simulation, the goal was simply to analyze the PLA hinges as all other stress calculations were already done in excel. From breaking the prototype once, we realized that the weakest point of the design is in the hinges, specifically where the structural rod lie in the large hinges (the hinges attached to the 13" and 18.5" end wood panels). Thus, for the simulation, the large hinges were simplified to cuboids with holes for the bolts, while inner hinges (hinges attached to the 7" middle panel) were neglected. These blocks were shortened so that there was no overhang of the 7" panel onto these blocks like there is in the final design. Instead, the 7" middle panel completely relied on the two structural rods. Bolts were also simplified to  $\frac{1}{4}$ " diameter rods with cylinder caps on each end representing the nuts. This was because we experienced many problems when using bolts and nuts.

**Fixed Geometries:** The 13" and 18.5" panels had 2"x3" extrusions representing where the axles would be attached. Since the only goal of this FEA was to analyze the PLA hinges, these extrusions were simply set as fixed geometries.

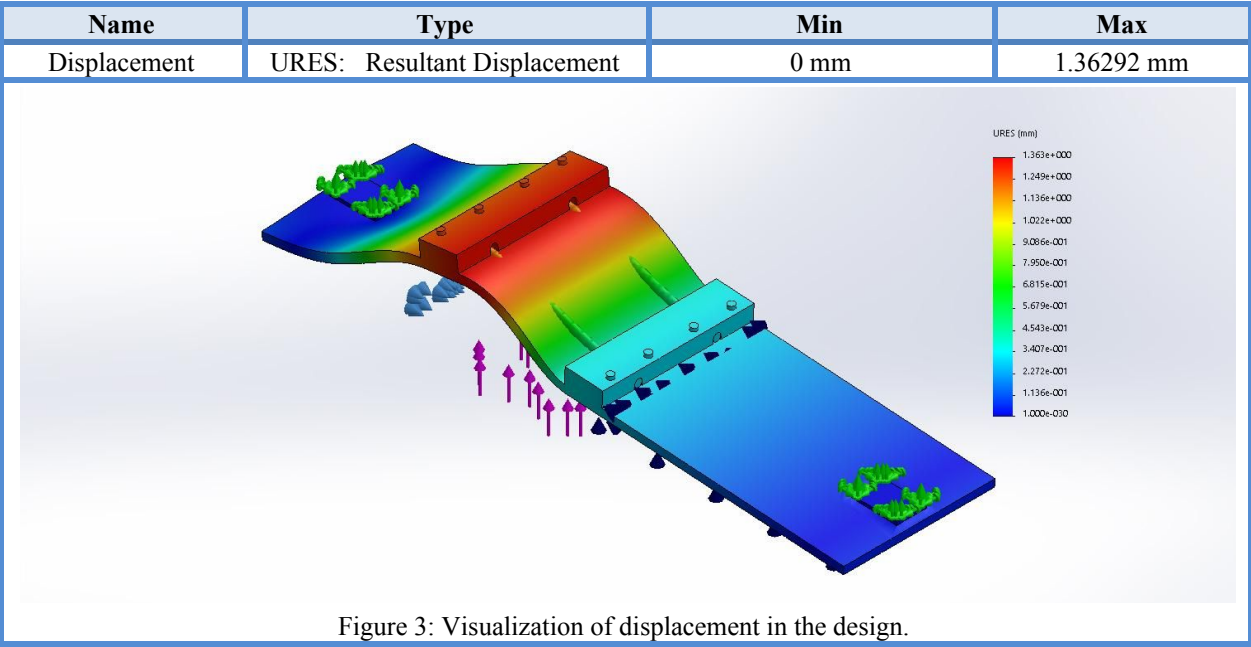
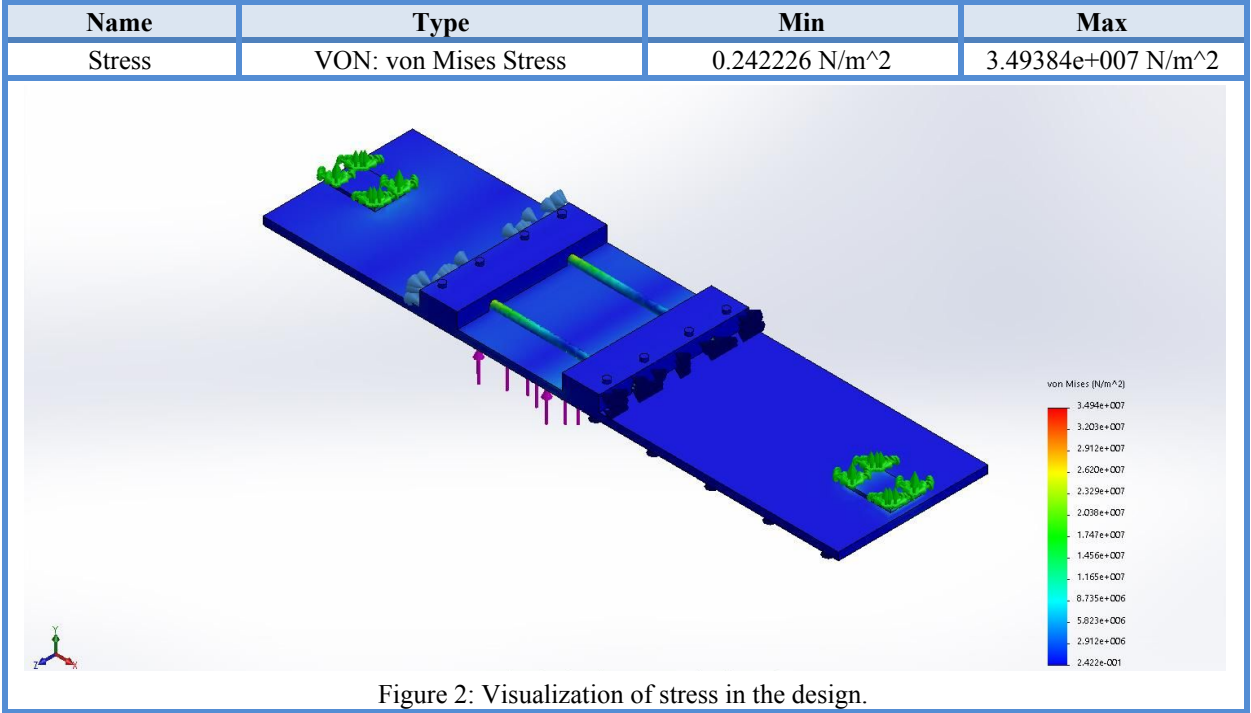
**Rigid Connections:** We initially thought of designing a way of keeping the rods in place in the hinges. However, from building out the prototype, the rods never shifted out of position because of how tight they were in the hinge. Thus, for the model, the ends of the structural rods were rigidly connected to the end face of the hinge blocks.

**Force:** A distributed force of 1128.15 N was applied to the center 7" middle panel.

**Materials:** The wood panels were modeled as Balsa. The structural rods were modeled as Aluminium 6061 because McMaster-Carr suggests using Aluminium 6061 to see the strength properties of carbon fiber. The hinge blocks were modeled as PLA. The bolts/nuts part were modeled as AISI 316 Annealed Stainless Steel.



Key Results



Part-Specific Max Stresses - Obtained through probing surfaces.

Max Von Mises in Structural Rods: 3.49e+07 Pa

Max Von Mises in Wood: 4.70e+06 Pa

Max Von Mises in PLA Hinges: 6.69e+06 Pa



## Appendix 4. Carbon Emissions Calculations

### Appendix 4.1. Carbon Emissions Calculation of Gasoline Car vs. Electric Longboard

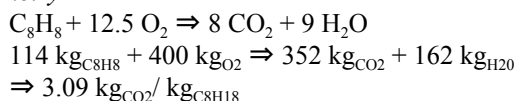
**Description:** Calculate the carbon dioxide equivalent emitted from a gasoline car versus and electric longboard over the mile range of the electric longboard (~4 miles). The electric longboard's measured rate of electricity mileage is 22.2 Wh/mile, using a 86.4Wh battery. This process, low-heating value (LHV), and molecular weight (MW) numbers come from an ME461 handout written by Professor Knight.<sup>33</sup>

1. Gasoline Car Scenario – Assumptions: The car's gasoline is purely octane.

- a. *Mileage*

US average gas mileage<sup>34</sup>=23.41mpg=8.072 mile/kg<sub>CH4H18</sub>  
(1 gallon of gasoline = 2.9 kg<sub>CH4H18</sub>)

- b. *Stoichiometry*



- c. *kg<sub>CO2</sub> emitted per unit distance traveled*

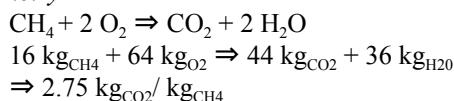
$$\begin{aligned} \text{kg}_{\text{CO}_2} / \text{distance} &= 3.09 \text{ kg}_{\text{CO}_2} / \text{kg}_{\text{C}_8\text{H}_{18}} \times 1/8.072 \text{ kg}_{\text{C}_8\text{H}_{18}} / \text{mile} \\ &= 0.383 \text{ kg}_{\text{CO}_2} / \text{mile} \end{aligned}$$

2. Electric Longboard Scenario – Assumptions: electricity used to charge the longboards' battery is produced from a power plant combusting methane. Methane leakage from distribution is neglected.

- a. *Mileage*

Measured mileage=22.2Wh/mile=0.0799 MJ/mile  
(1 Wh = 1/277.8 MJ)

- b. *Stoichiometry*



- c. *Energy supplied per unit kg<sub>CH4</sub>*

$$\begin{aligned} E_e &= \text{LHV } h_{\text{gen}} h_{\text{trans}} h_{\text{charge}} \\ &\sim 0.4 \text{ LHV} \\ &\sim 0.4 \times 52.2 \text{ MJ}_e / \text{kg}_{\text{CH}_4} \\ &\sim 20.9 \text{ MJ}_e / \text{kg}_{\text{CH}_4} \end{aligned}$$

- d. *kg<sub>CH4</sub> used per unit distance traveled*

$$\begin{aligned} \text{kg}_{\text{CH}_4} / \text{distance} &= 1/20.9 \text{ kg}_{\text{CH}_4} / \text{MJ}_e \times 0.0799 \text{ MJ}_e / \text{mile} \\ &= 0.00382 \text{ kg}_{\text{CH}_4} / \text{mile} \end{aligned}$$

- e. *kg<sub>CO2</sub> emitted per unit distance traveled*

$$\begin{aligned} \text{kg}_{\text{CO}_2} / \text{distance} &= 2.75 \text{ kg}_{\text{CO}_2} / \text{kg}_{\text{CH}_4} \times 0.00382 \text{ kg}_{\text{CH}_4} / \text{mile} \\ &= 0.0105 \text{ kg}_{\text{CO}_2} / \text{mile} \end{aligned}$$

3. Comparison: Over 4 miles, the gasoline fueled car emits 1.53 kg<sub>CO2</sub> while the electric skateboard (at the power plant) emits 0.0420 kg<sub>CO2</sub> (equivalent to 2.8% of the gas car's carbon emissions).

4. Adjusting Electric Longboard scenario to Florida's electricity generation source fuel mix (23% coal, 61% natural gas, 16% carbon-free sources).

- a. *Coal vs Gas Factor - assuming efficiencies are the same*

$$\begin{aligned} \frac{m_{\text{CO}_2 \text{ coal}}}{m_{\text{CO}_2 \text{ gas}}} &= \frac{\text{LHV}_{\text{gas}}}{\text{LHV}_{\text{coal}}} * \frac{\text{MW}_{\text{gas}}}{\text{MW}_{\text{coal}}} * \frac{M_c}{M_{\text{coal}}} \\ \frac{m_{\text{CO}_2 \text{ coal}}}{m_{\text{CO}_2 \text{ gas}}} &= \frac{52.2}{32.5} * \frac{16}{12} * 0.8 = 1.7 \end{aligned}$$

- b. *kg<sub>CO2</sub> emitted per unit distance traveled*

<sup>33</sup> Knight, Josiah. "GHG Emission from Battery-electric and Gas-Electric-Hybrid Vehicles: an Approximate Comparison". Handout. Duke University. Durham. 2017. Web.

<sup>34</sup> "Average Fuel Economy of Major Vehicle Categories." *US Department of Energy*, 2015. Available on <https://www.afdc.energy.gov/data/10310>

$$\begin{aligned}\text{kg}_{\text{CO}_2}/\text{distance} &= 0.61 (0.0105 \text{ kg}_{\text{CO}_2}/\text{mile}) + 0.23 (1.7 * 0.0105 \text{ kg}_{\text{CO}_2}/\text{mile}) \\ &= 0.0105105 \text{ kg}_{\text{CO}_2}/\text{mile} \\ &\sim = 0.0105 \text{ kg}_{\text{CO}_2}/\text{mile}\end{aligned}$$

## Appendix 4.2. Extrapolation of Carbon Emissions Savings for Case 1

Source used for data: 2015 Transportation Energy Databook.<sup>35</sup>

**Description:** Using Kaya equation for light duty vehicle (LDV) in the US and use these figures to estimate present annual LDV CO<sub>2</sub> emissions. Next, this model will be modified to predict the effect of a 2% adoption of our product in replacing LDV commutes under 5 miles long.

Assumptions:

- Since light duty vehicle diesel consumption is negligible in the US, all LDVs use gasoline.
- To increase the accuracy of the estimate, the calculations take into consideration both automobiles and light trucks/SUVs separately.

**Baseline:**

Estimate LDV Annual CO<sub>2</sub> Emissions (in metric tonnes/year):

$$\text{Population} * \text{PMT}/\text{pop} * [(\text{mileage-share}_{\text{car}} * \text{VMT}/\text{PMT}_{\text{car}} * \text{E}/\text{VMT}_{\text{car}}) + (\text{mileage-share}_{\text{truck}} * \text{VMT}/\text{PMT}_{\text{truck}} * \text{E}/\text{VMT}_{\text{truck}})] * \text{CO}_2/\text{E}$$

**Population:**

From TED Table 8.1: 316,498,000 people in 2013

**PMT/pop**

From TED Table 2.14 PMT for cars as 2,241,300 million miles/year in 2013, and 1,899,899 million miles/year for personal trucks (all 2013 values). Upon adding and dividing by population, the result is 13,084.44 miles/person.

**mileage\_share**

TED Table 2.12: the VMT for cars and personal trucks in 2012 was 1,446,800 and 1,032,554 million miles/year, respectively.

Thus, the mileage shares are  $\text{mileage\_share}_{\text{car}} = 0.58$  and  $\text{mileage\_share}_{\text{truck}} = 0.42$ .

**VMT/PMT**

TED Table 2.14 provides this ratio directly if you recognize that the load factor per vehicle (persons/vehicle) is the inverse of PMT/VMT. Hence,  $\text{VMT}/\text{PMT}_{\text{car}} = 0.65$  and  $\text{VMT}/\text{PMT}_{\text{truck}} = 0.54$  in 2013.

**E/VMT**

From TED Table 2.15,  $\text{E}/\text{VMT}_{\text{car}} = 4873 \text{ Btu}/\text{VMT}$  and  $\text{E}/\text{VMT}_{\text{truck}} = 6557 \text{ Btu}/\text{VMT}$  in 2013.

**CO<sub>2</sub>/E**

TED Table 11.11 tells us that the carbon content of gasoline is 19.6 lb CO<sub>2</sub>/gallon, and TED Table B.4 tells us that the energy content of gasoline is 115,400 Btu/gallon (net).

Convert lbs to tonnes to get  $\text{CO}_2/\text{E} = 7.70407\text{E-}08 \text{ tonne}/\text{Btu}$

Multiplying the terms through results in 1,060,571,188.11 tonnes CO<sub>2</sub>/year.

<sup>35</sup> Davis, Stacy. *Transportation Energy Data Book: Edition 36.1*. April 2018. Available on [cta.ornl.gov/data/index.shtml](http://cta.ornl.gov/data/index.shtml).

This is deemed a very reasonable result since it is within 1% of the reported value cited in Table 11.7 of the 2015 Transportation Energy Databook, which states that the actual LDV Annual CO2 Emissions figure was 1,065,800,000 metric tonnes/year in 2013.

To convert this data for use in **Case 1** of the environmental benefit analysis section of the paper, several figures are modified to assess the impact that our product would cause if it displaced 2% of drivers. It is acknowledged that this estimate will be a crude one, but provides a rough data point upon which insights on the impact of our product might be explained.

According to the National Household Travel Survey, around 60% of commutes are under five miles. If two percent of these commutes were displaced by our product, then 1.2% of LDV miles can be offset to characteristics of our product instead.

From calculations found on the *Carbon Emissions* section of the environmental benefit analysis, it is found that our products carbon emissions impact would be 1.8% of that of a gas car. This aligns with assumptions made earlier in this model. Together, the modified attributes lead to the calculation that a 2% adoption of our product for commutes under 5 miles would result in an annual LDV carbon emissions cut consisting of 1.17%, or 12,431,491 tonnes of CO2/year. The new estimated total LDV Annual CO2 Emissions (in metric tonnes/year) would thus be 1,053,368,508 tonnes of CO2/year.

#### Appendix 4.3. Table Listing Commuting Times Per Day

| Trip distance (miles) | Travel Day Vehicle Miles |                 |         |
|-----------------------|--------------------------|-----------------|---------|
|                       | Sample Size              | Sum (Thousands) | Percent |
| Less than 0.5 miles   | 31,851                   | 11,063          | 5       |
| 1 mile                | 98,955                   | 36,078          | 16.4    |
| 2 miles               | 84,856                   | 30,430          | 13.8    |
| 3 miles               | 64,205                   | 22,820          | 10.4    |
| 4 miles               | 48,361                   | 17,357          | 7.9     |
| 5 miles               | 37,449                   | 13,276          | 6       |
| 6 - 10 miles          | 106,830                  | 38,153          | 17.3    |

Source: National Household Travel Survey

#### Appendix 4.4. Extrapolation of Carbon Emissions Savings for Case 2

##### **Description:**

This calculation uses available data for Berlin to provide a reasonable estimate of the carbon savings associated with our product being adopted as a “last mile” solution by two percent of commuters who ordinarily travel via light duty vehicle (LDV). This assessment begins by first listing assumptions that were made, and important factors to consider. Next, calculations are conducted to arrive at the final estimate, which was designed to be conservative in nature.

##### **Assumptions and considerations:**

It is assumed that Berlin, Germany reflects other metropolitan areas around the world and the United States (such as Washington D.C.), where our product might also be adopted. Shortcomings of this assumption are briefly addressed

later in this section, and are not found to negate any findings. While using U.S. city data to conduct this assessment might better reflect the U.S. market, the decision to use Berlin is partially attributed to readily available data on its public transport.<sup>36</sup> Using a foreign market is acceptable since the product is not exclusive to domestic audiences, and can be adopted in developed markets beyond U.S. borders.

Two other significant forms of transport in Berlin include walking and biking, which are ignored in this assessment due to the lack of available data. The three sources considered for Berlin include LDV, bus, and rail transport.

This assessment assumes that kilometers travelled in an LDV vehicle for a certain commute is the roughly equivalent to the kilometers necessary for travelling in either a bus or rail. In the context of Berlin's robust public transportation network, this assumption was deemed justified and unlikely to produce significant error. This validity of this assumption was further strengthened by comparing public transport and vehicle routes in Berlin for six different trips, each roughly 5 miles long. In each case, the distances between were found to be within an average of 11% of one another, and thus close enough to one another to proceed with calculations. Nevertheless, the effect of this assumption is important to note, and might be worth further scrutiny in future studies in the form of a larger sample size in both Berlin and other metropolitan areas.

Another concern might be bus and rail capacity for accommodating additional commuters. This concern was neglected per assumptions made in the source of the Berlin data, which addressed the issue by citing how public transportation infrastructure in Berlin is capable of accommodating additional commuters.

It is predicted that the following calculations provide for a conservative estimate of the carbon savings associated with our products. One reason for the conservative nature of the prediction is because the "last-mile" aspect of the commuting journey with our product was neglected in this calculation. Instead, the calculation is done by offsetting personal vehicle transport with public transport methods (bus and rail), since the public transport portion of the commute is greater than the "last-mile" portion on our product. This aligns with the purpose of this calculation, which is to assess the impact of our product serving as a "last-mile" solution promoting the utility of existing public transportation networks. Recall the earlier finding in this report that our product provides for 1.8% of the carbon emissions of a gas car. With this finding in mind, it is easy to see how the inclusion of the "last-mile" portion of a commute on our product would serve to reflect even greater carbon savings than those calculated.

Another reason why the calculations in this assessment are a conservative estimate is because the calculations use data from the Berlin metropolitan area, where vehicles are far more fuel efficient than the US passenger vehicle fleet (35 vs. 23 mpg or 7.5 vs. 11.2 l per 100 km).<sup>37</sup> Overall, these two factors combine to strongly suggest that the carbon emission savings reflected in this assessment would be greater than 1.14% for the US market.

### **Baseline Calculation (*before our product is adopted*):**

KAYA: Transport GHG = Population \* PMT/Population \* VMT/PMT \* E/VMT \* GHG/E

Time period: 1 year

#### **LDV:**

$$CO_2 = 3,610,156 \text{ people} * \frac{2,607 \text{ km}}{1 \text{ person}} * \frac{1}{1.3} * \left( \frac{1.73 \text{ MJ}}{\text{vkm}} * \frac{7.31 \times 10^{-2} \text{ Kg CO}_2}{\text{MJ}} + \frac{0.424 \text{ MJ}}{\text{vkm}} * \frac{7.51 \times 10^{-2} \text{ Kg CO}_2}{\text{MJ}} \right) = 1,146,091,726 \text{ Kg CO}_2$$

#### **Bus:**

$$CO_2 = 3,610,156 \text{ people} * \frac{471.5 \text{ km}}{1 \text{ person}} * 0.05181 * \frac{16.57 \text{ MJ}}{\text{vkm}} * \frac{7.51 \times 10^{-2} \text{ Kg CO}_2}{\text{MJ}} = 109,744,737 \text{ kg CO}_2$$

#### **Rail:**

<sup>36</sup> Fulton, Kevin, and Iberkak, Ismail. *Berlin Transportation System Analysis*. December, 2016. TS. Duke University. Available on <https://drive.google.com/file/d/0B0NmybeAdbOHSIBBM3FzYm5CSGs/view?usp=sharing>

<sup>37</sup> Buehler, Ralph, and John Pucher. "Urban Transport: Promoting Sustainability in Germany." *Lessons from Europe?: What Americans Can Learn from European Public Policies*, pp. 139–162., doi:10.4135/9781483395357.n8.

$$CO_2 = 3,610,156 \text{ people} * \frac{9,425.16 \text{ km}}{1 \text{ person}} * 0.00204 * \frac{11.57 \text{ kWh}}{\text{vkm}} * \frac{.6 \text{ kg CO}_2/\text{kwh} \text{ Kg CO}_2}{\text{kWh}} = 481,869,543 \text{ kg CO}_2$$

$$\text{Total CO}_2 = 1,737,706,006 \text{ kg CO}_2$$

$$\text{LDV: } 3,610,156 \text{ people} * \frac{2,607 \text{ km}}{1 \text{ person}} = 9,411,676,692 \text{ km from entire current Berlin city population.}$$

$$\text{Bus: } 3,610,156 \text{ people} * \frac{471.5 \text{ km}}{1 \text{ person}} = 1,702,188,554 \text{ km from entire current Berlin city population}$$

$$\text{Rail: } 3,610,156 \text{ people} * \frac{9,425.16 \text{ km}}{1 \text{ person}} = 34,026,297,925 \text{ km from entire current Berlin city population}$$

If we offset 2% of the light duty vehicle (LDV) driving commuters: A 2% decrease in kilometers travelled would lead to an annual total 9,223,443,158 km travelled via LDV vehicle. Per stated assumptions, commuters must now offset the 188,233,534 km through public transportation methods in bus and rail.

### **Future Calculation (after our product's adoption amounts to 2% of LDV miles travelled):**

With constant proportionality in mind, it is found that 5% of the 188,233,534 km would be allocated to bus transport, while the remainder would be allocated to rail transport. To arrive at a modified form the kilometers travelled per person via bus and rail forms of transport, the following calculations are conducted:

$$\text{Bus: } 9,411,676.7 \text{ km} + 1,702,188,554 \text{ km} = 1,711,600,230 \text{ km}$$

$$1,711,600,230 \text{ km} \div 3,610,156 \text{ people} = 474.1/1 \text{ person}$$

$$\text{Rail: } 178,821,857.3 \text{ km} + 34,026,297,925 \text{ km} = 34,205,119,800 \text{ km}$$

$$34,205,119,800 \text{ km} \div 3,610,156 \text{ people} = 9474.7 \text{ km/ 1 person}$$

As stated earlier, the desired output is the effect of our product's adoption on carbon emissions. Finding this desired output can be accomplished by plugging in the modified inputs into the KAYA equation again.

$$\text{KAYA: Transport GHG} = \text{Population} * \text{PMT/Population} * \text{VMT/PMT} * \text{E/VMT} * \text{GHG/E}$$

#### **LDV:**

$$CO_2 = 9,223,443,158 \text{ km} * \frac{1}{1.3} * \left( \frac{1.73 \text{ MJ}}{\text{vkm}} * \frac{7.31 \times 10^{-2} \text{ Kg CO}_2}{\text{MJ}} + \frac{0.424 \text{ MJ}}{\text{vkm}} * \frac{7.51 \times 10^{-2} \text{ Kg CO}_2}{\text{MJ}} \right) = 1,123,169,891 \text{ Kg CO}_2$$

#### **Bus:**

$$CO_2 = 3,610,156 \text{ people} * \frac{474.1 \text{ km}}{1 \text{ person}} * 0.05181 * \frac{16.57 \text{ MJ}}{\text{vkm}} * \frac{7.51 \times 10^{-2} \text{ Kg CO}_2}{\text{MJ}} = 110,349,904 \text{ kg CO}_2$$

#### **Rail:**

$$CO_2 = 3,610,156 \text{ people} * \frac{9,474.7 \text{ km}}{1 \text{ person}} * 0.00204 * \frac{11.57 \text{ kWh}}{\text{vkm}} * \frac{.6 \text{ kg CO}_2/\text{kwh} \text{ Kg CO}_2}{\text{kWh}} = 484,402,318 \text{ kg CO}_2$$

$$\text{Total CO}_2 = 1,717,922,113 \text{ kg CO}_2$$

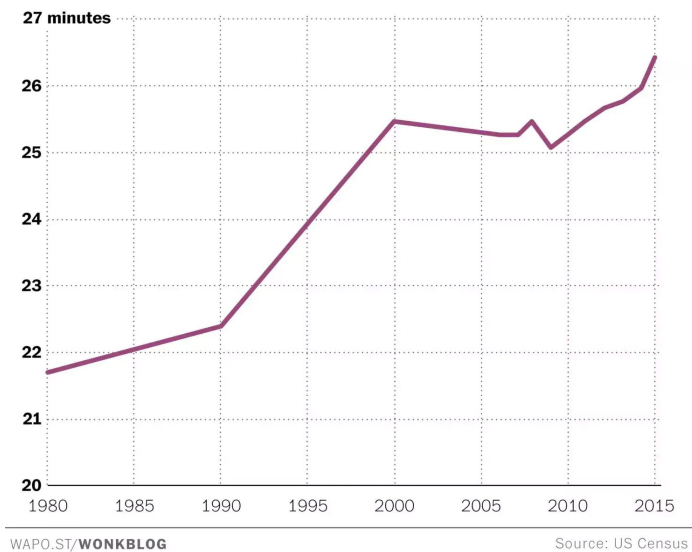
If two percent of vehicle miles travelled via LDV are offset to public transportation due to our product's positioning as a "last-mile" solution, the carbon savings are found by taking the difference between the original scenario, and the predicted scenario:

$$1,737,706,006 \text{ kg CO}_2 - 1,717,922,113 \text{ kg CO}_2 = 19,783,893 \text{ kg CO}_2, \text{ or a 1.14\% reduction.}$$

## Appendix 4.5. Graph of Rising American Commute Times

### The American commute keeps getting longer

Average travel time to work, 1980 – 2015



Source: The Census 2015 American Community Survey data<sup>38</sup>

<sup>38</sup>Ingraham, Christopher. "Analysis | The American Commute Is Worse Today than It's Ever Been." *The Washington Post*, WP Company, 22 Feb. 2017, [www.washingtonpost.com/news/wonk/wp/2017/02/22/the-american-commute-is-worse-today-than-its-ever-been/?noredirect=on&utm\\_term=.67235d5e96ef](http://www.washingtonpost.com/news/wonk/wp/2017/02/22/the-american-commute-is-worse-today-than-its-ever-been/?noredirect=on&utm_term=.67235d5e96ef).

## Appendix 5. Bill of Materials for Full Project Progress

| Item                      | Description   | Quantity | Date Ordered | Price             |
|---------------------------|---|----------|--------------|-------------------|
| Plywood                   | 1/2" thick, 2' x 4' sanded plywood  | 2        | 1/22/18      | \$26.00           |
| Motor                     | 6355 190kV Motors, 2500W, 2.83Nm  | 2        | 1/22/18      | \$180.00          |
| Dual Motor Mechanical Kit | 83mm wheels (2), trucks (2), 1/4" truck risers, fasteners, drivetrain*                        | 1        | 1/22/18      | \$199.00          |
| Battery                   | 6S2P Electric Skateboard EPower Battery Pack  | 1        | 2/2/18       | \$185.00          |
| VESC                      | Torque ESC VESC Electronic Speed Controller   | 1        | 2/2/18       | \$99.99           |
| Remote                    | 2.5 GHZ Remote Controller   | 2        | 2/2/18       | \$120.00          |
| Servo-Connector           | Male-male connection, connects VESC to RC Receiver  | 1        | 2/2/18       | \$1.99            |
| Fasteners                 | Screws, Locknuts, Washers -- 1/4" and 5/16" **  | 2        | 3/1/18       | \$10.82           |
| Ratchet                   | 3" OD, 3/8" thick, 48 teeth, stainless steel  | 1        | 3/1/18       | \$55.88           |
| Pawl                      | 1 5/16" long, 3/8" thick, stainless steel   | 1        | 3/1/18       | \$46.54           |
| Wire Rope                 | 1/8" thick, 3/16" coating OD, 3' long, weather-resistant coated, galvanized steel, 400lb cap. | 3        | 3/1/18       | \$6.12            |
| Maple Veneers             | 1/16" thick (2), 1/8" thick (1), 1/4" thick (1); 8" x 24"                                     | 1        | 3/1/18       | \$49.00           |
| Maple Veneers             | 1/4" thick (3), 1/8" thick (2), 1/2" thick (1); 10"x24"                                       | 1        | 3/5/18       | \$84.50           |
| Bluetooth Receiver        | Adafruit Bluetooth LE UART Friend   | 1        | 3/19/18      | 17.50             |
| Ratchet Straps            | 1-1/4 in x 16ft Ratchet Tie-Down (4-Pack)   | 1        | 3/23/18      | \$17.96           |
| Steel Rods                | 1/4"-20 Steel Rods, 10" long  | 15       | 3/26/18      | \$34.20           |
| Fasteners 2               | Screws, Locknuts -- 1/4"-20 and 10-24   | 1        | 4/5/18       | \$20.55           |
| Carbon Fiber Rods         | Carbon Fiber Rod, 1/2" Diameter, 12" Long   | 2        | 4/9/18       | \$47.96           |
| Ratchet Hinges            | 80/20 Inc., 12085, 15/40/45 Series, Standard Hinge with Locking Lever                         | 4        | 4/2/18       | \$66.34           |
|                           |   |          | <b>Total</b> | <b>\$1,269.35</b> |

\*Drivetrain includes 2 of each of the following: motor mount, drive wheel pulley, motor pulley, and timing belt.

\*\* Many other bolts and nuts used were provided as spares from Patrick McGuire in the MEMS department

## Appendix 6. Bill of Materials for Final Design

| Item                      | Description  | Quantity | Price           |
|---------------------------|--|----------|-----------------|
| Motor                     | 6355 190kV Motors, 2500W, 2.83Nm   | 1        | \$90.00         |
| Dual Motor Mechanical Kit | 83mm wheels (2), trucks (2), 1/4" truck risers, fasteners, drivetrain*   | 1        | \$199.00        |
| Battery                   | 6S2P Electric Skateboard EPower Battery Pack   | 1        | \$185.00        |
| VESC                      | Torque ESC VESC Electronic Speed Controller  | 1        | \$99.99         |
| Remote                    | 2.5 GHZ Remote Controller  | 1        | \$60.00         |
| Servo-Connector           | Male-male connection, connects VESC to RC Receiver   | 1        | \$1.99          |
| Maple Veneers             | 1/2" thick (2); 10"x24"  | 1        | \$42.00         |
| Steel Rods                | 1/4"-20 Steel Rods, 10" long   | 2        | \$4.16          |
| Carbon Fiber Rods         | Carbon Fiber Rod, 1/2" Diameter, 12" Long  | 2        | \$47.96         |
| Fasteners                 | 1/4-20 Phillips Flat Head Screws 2" long, 4-40 Phillips Flat Head Screws 7/8" long, 1/4-20 Locknuts, 4-40 Locknuts | 1        | \$23.96         |
| PLA Plastic               | 1kg spool of PLA plastic. Total PLA parts weighs 1.0kg.  | 1        | \$28.01         |
| <b>Total</b>              |  |          | <b>\$782.07</b> |

\*Although only one motor is used in the final design, the dual motor mechanical kit is cheaper than buying the drivetrain, wheel and trucks separately (which would total to \$207). This dual motor mechanical kit's drivetrain includes 2 of each of the following: motor mount, drive wheel pulley, motor pulley, and timing belt.